



ISTITUTO NAZIONALE DI FISICA NUCLEARE

Sezione di Napoli

INFN/TC-00/23
21 December 2000

**STATUS OF THE HIGH CURRENT PROTON ACCELERATOR
FOR THE TRASCO PROGRAM**

The TRASCO_AC Group

Abstract

TRASCO (the acronym for TRAsmutazione di SCOrie, which stands for waste transmutation) is a joint INFN/ENEA program aiming at the design and the technological investigation of the main components of an accelerator driven system (ADS) for nuclear waste transmutation. We discuss here the status of the R&D activities on the high current proton accelerator, under INFN responsibility.

PACS.: 29.17.+w, 29.27.-a

*Published by **SIS-Pubblicazioni**
Laboratori Nazionali di Frascati*

The TRASCO_AC Group:

R. Ballantini^a, D. Barni^b, R. Baruzzo^c, G. Basoni^d, A. Bazzani^e, G. Bellomo^b, G. Bisoffi^f,
M. Bonezzi^b, A. Bosotti^b, C. Campisano^g, L. Celona^h, C. Chemelliⁱ, G. Ciovati^b,
F. Chines^h, G. Ciavola^h, M. Comunian^f, A. Conte^j, G. Corniani^d, A. Daccà^a,
A. Emmanouilidis^a, A. Facco^f, M. Fusetti^b, S. Gammino^h, G. Gemme^a, C. Gesmundo^b,
G.V. Lamanna^k, A. Lombardi^f, S. Marletta^h, P. Michelato^b, M. Napolitano^l, R. Parodi^a,
A. Palmieri^f, C. Pagani^b, G. Penco^b, P. Pierini^b, A. Pisent^f, S. Rambaldi^e, E. Robert^h,
F. Scarpa^f, V. Stagno^k, G. Turchetti^e, V. Variale^k, G. Varisco^b, V. Zviaginste^f

^aINFN Sezione di Genova, Via Dodecaneso 33, I-16146 Genova, Italy

^bINFN Sezione di Milano – LASA – Via Fratelli Cervi, 201, I-20090 Segrate (MI), Italy

^cCINEL Strumenti Scientifici, Via Dell'Artigianato 14, I-35010 Vigonza (PD), Italy

^dZANON, Via Vicenza 113, I-36015 Schio (VI), Italy

^eUniversity of Bologna, INFN Sezione di Bologna, Via Irnerio 46, I-40126, Bologna, Italy

^fINFN Laboratori Nazionali di Legnaro, Via Romea 4, I-35020 Legnaro (PD), Italy

^gHitec, Via G. Arcoleo 2, Gravina di Catania, I-95030 Catania, Italy

^hINFN Laboratori Nazionali del Sud, Via S. Sofia 44, I-95123 Catania, Italy

ⁱCESI, Via Rubattino 54, I-20134 Milano, Italy

^jSAES Getters, Viale Italia 77, 20020 Lainate (MI), Italy

^kINFN Sezione di Bari, Via E. Orabona 4, I-70126 Bari, Italy

^lINFN Sezione di Napoli, Via Cintia, I-80126 Napoli, Italy

1 INTRODUCTION

The disposal of radioactive wastes resulting from industrial nuclear energy production (and from the nuclear weapons dismantling) represents a problem which is not yet fully solved, especially in terms of environmental and social acceptability.

The Deep Geological Repository seems to be the only possible final solution, however, in order not to leave a heavy heritage to future generations, there is the need for finding ways to drastically reduce the volumes and the radio toxicity of the High Level Waste to be stored and the time needed to reach the radioactivity level of the natural ores originally used for the fuel production.

Partitioning and transmutation (P/T) technologies could allow reaching these goals. The most hazardous material – i.e. plutonium, minor actinides (MA) and some long-lived fission products (FP) – would be separated (partitioning) from the nuclear wastes and, then, converted (transmutation) to shorter lived elements in specially designed reactors. Transuranics would be transmuted by fission and FP by neutron capture and beta decay.

Even though a critical reactor (burner reactor) could be considered as potential candidate as dedicated transmutation system, systems loaded with mostly MA based fuel suffer from safety problems related to their reactivity coefficients (increase in the void reactivity coefficient and decrease in the Doppler effect) and to a small value of the delayed neutron fraction.

Therefore, the characteristics of an accelerator driven system (ADS) - a sub-critical reactor coupled to a spallation neutron source driven by a high power proton accelerator - are particularly suited, especially to mitigate the latter problem, and allow reaching the maximum transmutation rates while maintaining an intrinsically safe operation.

For these reasons, recently ADS systems have become a major R&D topic in Europe. The resources presently allocated are significant and are related to a large number of activities, spanning from accelerator and reactor system design to material and fuel technologies. The organizations undertaking these activities range from national R&D bodies to Universities, with a significant participation of several major nuclear industries of the European countries. In some countries, specifically coordinated national programs have been defined and a few experimental facilities, either for the driver accelerator or for the sub-critical assembly, are under construction or in the planning phase.

Important ADS activities are also going on or are being planned outside Europe e.g., in Japan - the JAERI and KEK Joint Project ¹⁾ - and USA - the AAA project ²⁾. In both cases, the programs are relevant both in terms of R&D resources and in terms of planned test facilities realization.

Important spin-offs of ADS activities outside the field of waste transmutation have been identified, such as development of high intensity accelerators - for spallation neutron sources and their applications - liquid metal technology, new structural materials, radioisotopes production, actinide chemistry etc.

1.1 The Italian program TRASCO

Starting from 1996, a growing interest on the Accelerator Driven Systems concepts has taken place in Italy and has given origin to several studies. The basic R&D program TRASCO³⁾ has been approved at the governmental level and has been funded by MURST (the Ministry of the University, Scientific and Technological Research) and two participating institutions on almost equal bases, and has been followed by an industrial program, in which major Italian research institutions and industries are involved.

TRASCO aims to study the physics and to develop the technologies needed to design an Accelerator Driven System (ADS) for nuclear waste transmutation and was initially prepared with close reference to Carlo Rubbia's Energy Amplifier proposal⁴⁾.

The TRASCO program consists of two main parts, regarding, respectively, the accelerator and the sub-critical system. The first part falls under the competencies of INFN (the National Institute for Nuclear Physics) and the second under those of ENEA (the National Agency for New Technologies, Energy and Environment), which are the two institutions jointly responsible of the TRASCO activities, which include also Italian industrial partners. This program is considered of particular relevance for the creation of a well-mixed group of competencies and it will provide results of relevant importance in support of any related industrial program.

The project covers all the main subsystems of an ADS (accelerator, window/target, sub-critical reactor). However, due to the limited available financial resources, all the efforts are concentrated on starting some significant and qualified experimental activities, in view of the goal of a future participation in an International project for the study and construction of an ADS prototype, like the Energy Amplifier for waste transmutation.

The main objectives of the research program can be summarized by the following short items:

- A conceptual design of a 1 GeV - 30 mA proton linear accelerator (linac);
- The design and construction of the proton source and of the first section of the radio frequency quadrupole (RFQ) pre-accelerator, as well as of some prototypical cavities for the super-conducting high energy section of the linac;
- The development of methods and criteria for the neutronics, the thermal-hydraulics and the plant design for an EA/ADS sub-critical system, as well as specific aspects related to the safety analysis of this type of nuclear installation;
- The materials technologies and the development of components to be used in a plant in which lead or lead-bismuth acts both as a primary target and as a coolant;
- The experiments to validate and verify proposed technologies for materials compatibility with lead and lead-bismuth alloys.

Besides ENEA and INFN, the program involves some qualified Italian firms and other Italian public research institutions (namely, Universities and INFN, the National Institute for Physics of Matter).

The following nine research sub-programs have been set for TRASCO. The research groups indicated between brackets - involving both research institutes and firms – are responsible of the following sub-programs:

1. Proton source (INFN, SISTEC, HITEC);
2. Low and medium energy accelerator section (INFN, CINEL);
3. High energy accelerator section (INFN, CISE, SAES-Getters, ZANON);
4. Neutron production for material characterisation (INFN, INFM);
5. General safety criteria and classification (ENEA, ANSALDO)
6. Neutronics and transmutation efficiency (ENEA, CIRTEN, CRS4, University of Bologna);
7. Thermal-hydraulic analysis (ENEA, CIRTEN, CRS4, ANSALDO);
8. Beam window technology (ENEA, CIRTEN, ANSALDO, INFM);
9. Materials technology and compatibility with Lead and/or Lead-Bismuth alloy (ENEA, CIRTEN, CRS4, FN, ANSALDO).

In this paper we describe only the objectives and status of the accelerator activities of the TRASCO_AC program (i.e. the sub-programs from 1 to 3 in the previous list).

1.2 TRASCO_AC, the accelerator studies for TRASCO

A short description of the layout of the accelerator under study for the TRASCO_AC program is given briefly below. In the next sections the status of the activities will be presented more thoroughly.

1.2.1 Proton source

High intensity proton sources of several tens of mA already exist – at Chalk River National Laboratory, at Los Alamos National Laboratory (LANL), and at CEA-Saclay – but additional R&D efforts are still necessary for ensuring the availability and reliability required by the ADS system. ⁵⁾

The objectives of this sub-program are the feasibility study, design, construction and test of a 2.45 GHz microwave source that can produce 35 mA dc proton beam with a normalized emittance below 0.2π mm mrad for an operating voltage of 80 kV.

Taking into account the state-of-the-art of such devices, some R&D is needed for achieving the required current and voltage stability, as well as a satisfactory controlled low beam emittance.

The conceptual design carried for the TRASCO program addressed all the parts of the source and included the beam matching with the RFQ, which constitutes the first part of the following linac.

The final design benefits of the experience gained with the source SILHI of CEA/Saclay⁶⁻¹¹); construction and test of the TRIPS (TRAsco Intense Proton Source) source have followed these preliminary activities and the improvements which have been studied in the frame of the TRASCO project have represented a significant step forward. At last, an extended optimization of the main components of the source has been carried out for achieving the best compromise between different parameters (proton fraction, electronic density, emittance, etc.).¹²⁻¹³

1.2.2 Low and Medium Energy Accelerator Section

The final goal of this sub-program is the complete conceptual design of the linac portion up to the energy of about 100 MeV, for a nominal proton current of 30 mA. The medium energy linac injects the beam in the CW super-conductive linac, which will be described in the next section.

The sub-program includes the design and construction of prototypes of some critical components.

Three different options have been analyzed and compared:

- a) A normal-conductive, continuous-wave RFQ (up to 5 MeV) followed by a standard Drift Tube Linac (DTL) at 352.2 MHz;¹⁴
- b) A normal-conductive CW RFQ followed by two-gap, $\lambda/4$ or $\lambda/2$, super-conducting cavities at 176 MHz or 352.2 MHz;¹⁵
- c) A normal-conductive CW RFQ followed by super-conductive elliptical reentrant cavities at 352.2 MHz.¹⁶⁻¹⁸

This sub-program included the construction of a full-scale aluminum mock-up of the RFQ for RF tests at low power¹⁹) and, after the engineering validation phase - now in progress - the construction of a full-scale section of the RFQ, in which both low and high power tests will be performed.²⁰⁻²⁴) Beam halo studies complete the activities.²⁵⁻²⁸)

As far as the development of a super-conductive reentrant cavity for the medium energy section is concerned, a niobium prototype is under fabrication. At the same time the architecture study of the linac and the beam dynamics studies are advanced, while a 500 W module of a modular 352MHz solid-state amplifier is under development.

1.2.3 High energy accelerator section

The high-energy section of the linac accelerates the proton beam from 100 MeV to approximately 1 GeV (and possibly to higher energies), thus representing the biggest and most expensive component of the accelerator.

The design of this part of the linac is based on super-conductive elliptical type accelerating structures. Two operating frequencies have been considered and extensively compared for the design: the LEP II (CERN) 352.2 MHz frequency²⁹⁻³⁵) and its doubled

value of 704.4 MHz.³⁶⁻⁴³⁾ Due to the fact that the proton beam at these energies is still varying its longitudinal velocity during the acceleration, three different families of β -graded multicell cavities^{44,45)} are foreseen along the linac, corresponding to matched β of about 0.5, 0.68 and 0.86, respectively. The choice of the operating frequency implies a different choice of fabrication technology for the superconducting cavities: for the LEP 352.2 MHz it is possible to use the relatively “cheap” Nb sputtering on copper cavities – that has been proven to be able to provide acceleration gradients of about 8 MV/m for cavity with a β close to unity – while the 704.4 MHz allows to take advantage of the outstanding performances of the bulk Nb cavities set by the recent developments driven by the TESLA/TTF Collaboration. Both technologies have been investigated in the prototypical activities of the TRASCO program.

This sub-program concerns the conceptual design and the beam dynamics⁴⁶⁻⁵⁰⁾ analysis of the whole super-conductive linac (with an energy extension up to approximately 2 GeV), as well as the development and construction of prototypical superconductive cavities.^{51,52)}

The first part of the sub-program, while defining the general layout of the accelerator, has been particularly focused on the detailed study of:

- a) A comprehensive electromagnetic and mechanical design of the accelerating structures;⁵³⁾
- b) The assessment of the thermal and mechanical performances of the structures;
- c) The beam dynamics and halo problems, with the goal of minimizing the particle losses.

The design, construction and test of typical SC cavities at both frequencies, as well as the development of the cryostat design has been the objective of the second part of the activity, now under completion. In particular, a single cell bulk Nb 704.4 MHz cavity at the lowest $\beta=0.5$ has been constructed and tested, and both a single cell and a complete five-cell – at 352.2 MHz - Nb sputtered on copper structure at the highest $\beta=0.85$ has been fabricated and tested in cooperation with CERN.⁵²⁾

As part of the beam dynamics activities a dedicated code with 3D space charge modeling capabilities^{46,49)} has been written for the specific case of simulating high-current proton beams in elliptically shaped superconducting cavities. This activity has been driven by the requirement of keeping the beam losses below 1 nA/m in order to limit the accelerator activation and to reduce dose rates at personnel during maintenance.

1.3 Overall status of TRASCO

The TRASCO program officially started in 1998 and a number of activities have been carried out both on the accelerator and the sub-critical system.

A reference conceptual design of the proton source and medium energy section - the 352.2 MHz RFQ and a DTL - has been determined, for a nominal accelerated current of

more than 30 mA. The TRIPS source has been built and has already delivered the beam in LNS. A detailed design and engineering work of the RFQ has started and a 3 m long aluminum model of the RFQ has been built and measured for RF field stabilization tests.

Preliminary studies of an Independently Phased Superconducting Cavity Linac (ISCL) - to be used instead of the traditional DTL - have been also done. The ISCL is similar to the accelerators used for low energy heavy ions in several nuclear physics laboratories, as the Italian LNL. In the present case the structures need to be designed for much higher beam intensities and for wider particle velocity ranges. Various approaches have been checked, like single and double gap cavities, at the frequencies of 176 and 352.2 MHz. The most promising design of a 352.2 MHz ISCL ranging from 5 MeV up to 100 MeV, is based on the so-called “reentrant cavities”, that are modified cylindrically symmetric pillbox cavities and, therefore, theoretically guaranteed to be dipole free. Many points of this design work are preliminary but will be used for cavity R&D activities.

The conceptual design of the 352.2 MHz superconducting LINAC, able to bring the 30 mA proton beam from 100 MeV up to 1700 MeV, has already been worked out and is mostly based on the LEP II technology. The design foresees three different sections with transition energies at 190 and 430 MeV. A doublet array structure, with cavities placed in the long drift space between the quadrupoles will provide the necessary transverse focusing. The three sections will employ 2, 3 and 4 five-cell cavities per focusing period, respectively. The design of the cavities has been performed investigating carefully all the electromagnetic and structural performances. The construction and the tests of the Nb-sputtered copper $\beta=0.85$ single-cell and multi-cell prototypes cavities has been done at CERN, under a collaboration agreement between CERN and INFN.

Starting from a study of linac design frequency scaling laws, and in order to take advantage of the bulk Nb cavity fabrication technology set by in the last few years by the TESLA/TTF International Collaboration - in which INFN is involved with the same group of Milano participating in TRASCO - a linac design based on the use of 704.4 MHz frequency for a superconducting section from about 100 MeV to nearly 2 GeV and for beam currents in excess of 30 mA has been carried out. The choice of bulk niobium cavities allowed increasing the cavity gradients and shortening the superconducting linac length by nearly a factor 2. The smaller physical dimensions of the cavities - due to the higher frequency - also reduce by a great amount the cost of the prototype activities - less niobium needed, infrastructure dimensions for fabrication and testing are smaller. Further pros and cons of the two frequency choices will be presented later in this paper.

2 THE TRASCO INTENSE PROTON SOURCE: TRIPS

The design of the TRASCO intense proton source (TRIPS) has been completed in 1999 and the source has been assembled at LNS in May 2000.

Its task consists of the production of 35 mA dc proton beam with a normalized emittance below 0.2π mm mrad for an operating voltage of 80 kV. The source is based on the principle of microwave discharge, off-resonance, and it is a modified version of the source SILHI operating at CEA/Saclay since four years⁸⁾.

With respect to that source some things have been changed and some new features have been added: the microwave matching system has been modified in a four step maximally flat transformer^{54,55)}, a system to move the coils on-line has been implemented, but mainly the efforts have been concentrated on the extraction system with the aim to increase the source availability and reliability, in order to meet the requirement of a driver for an ADS system.

The main features of the source have been defined by taking in considerations the needs of the highest possible reliability (few failures per year).

The choice of an off-resonance microwave discharge ion source has been motivated by the requirements of high yield, high proton fraction and long term stability.

The results obtained with measurements at the proton source SILHI in Saclay confirmed that the currents and voltages at which the TRIPS design aims can be reliably achieved, and that low beam emittances can be obtained by means of controlled gas injection in the beamline^{6,7)}.

Therefore the major developments to be done at LNS will concern stability, reliability and reproducibility.

2.1 The TRIPS design

The design of TRIPS is shown in FIG. 1. The microwave power obtained with a 2.45 GHz - 2 kW magnetron is coupled to the cylindrical water-cooled OHFC copper plasma chamber (100 mm long and 90 mm in diameter) through a circulator, a four stub automatic tuning unit and a maximally flat matching transformer. The microwave pressure window is placed behind a water-cooled bend in order to avoid any damage due to the back-streaming electrons.

Two magnetic coils, independently on-line moved and energized in order to vary the position of the electron cyclotron resonance (ECR) zones in the chamber, produce the desired magnetic field configuration.

Moreover, the design has been aimed to simplify the operations of maintenance especially in the extraction zone.

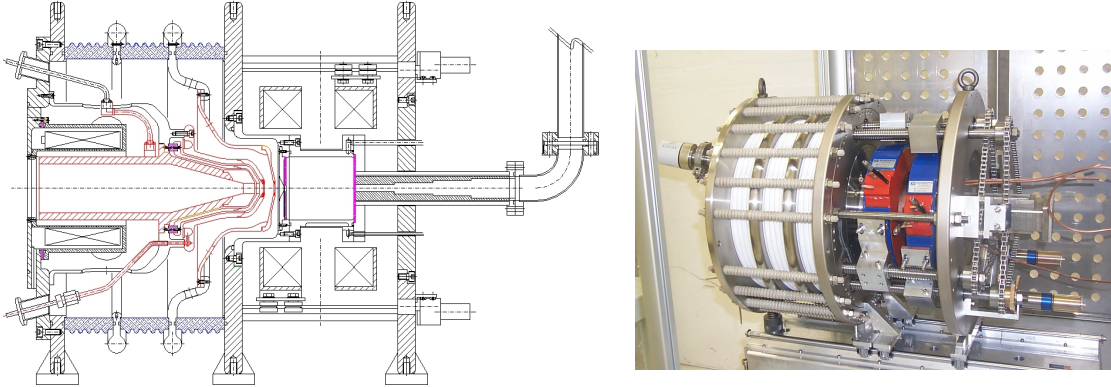


FIG. 1: A drawing of TRIPS (left) and the source installed on the HV platform (right).

2.2 The matching transformer

In order to optimize the coupling between the microwave generator and the plasma chamber a multisection quarter-wave transformer is used⁵⁴⁾ (FIG. 2).

In our application the impedance of a WR284 waveguide working in the dominant mode (TE₁₀ mode) is to be matched to the equivalent impedance of plasma.

For our purposes we have chosen to use a four step binomial matching transformer that will be inserted immediately ahead of the microwave window.

The transformer realizes a progressive match between the two impedances Z_0 and Z_5 and concentrates the electric field at the center of the plasma chamber (in our design the field enhancement ratio is around 2). The overall result is a significant increase of the extracted current density as we have observed during the commissioning of the source MIDAS2 which uses the same type of matching unit.⁵⁵⁾

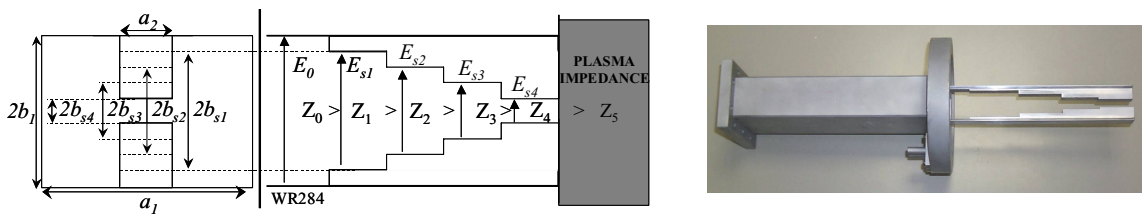


FIG. 2: A sketch of the double ridged binomial transformer (left) and its picture (right).

2.3 The extraction geometry design

The extraction geometry of the TRIPS source is the result of several studies on the SILHI extraction system conducted in collaboration with the CEA team and with J. Sherman of Los Alamos National Laboratory.

Different topologies have been investigated in order to increase the reliability of the SILHI source ^{9,11}). The main configurations studied were: the tetrode (already used at LANL) and the pentode (currently used on SILHI); all the simulations have been carried out with the AXCEL code, the results have been cross checked with the IGUN code and with the PBGUN code with a collaboration of J. Sherman.

The configuration chosen for SILHI was the pentode, and in the last two years different solutions have been tested on the source according to the calculations done.

The last configuration calculated permitted to obtain in the long run test of 104 h (October 99) the outstanding availability of 99.96% (only one spark occurred).

The final design of the extraction system of TRIPS benefits of this knowledge and experience acquired: because the operational voltage of TRIPS is 80 kV (instead of 95 kV of SILHI), the extraction system was redesigned and the electrode geometry has been varied.

The gaps, the voltage and the extraction holes have been modified in order to reduce the length of the extraction zone where the beam is uncompensated and to reduce the aperture-lens effect.

Also in this case beam dynamics simulations have been performed with the AXCEL code and the results have been crosschecked with the IGUN code.

RMS normalized emittance below 0.2π mm mrad (including the beam halo) have been calculated. The trajectory plot of the extraction system of TRIPS is shown in FIG. 3.

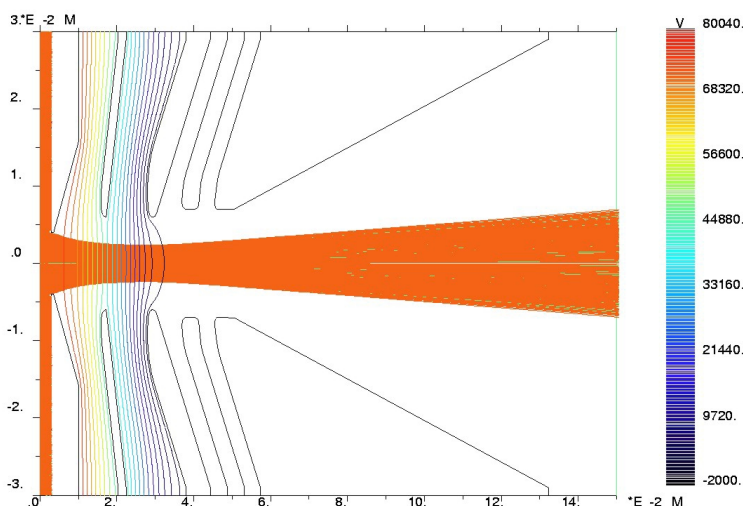


FIG. 3: Trajectory plot of the TRIPS extraction system: the extraction voltage is 80 kV and the puller voltage is 45 kV.

Finally, the electrodes are split in two parts (FIG. 4): this feature will permit a fast replacement and easy modifications of the extraction optics without changing the electrodes' mechanical support.



FIG. 4: The extraction electrodes.

2.4 The source status

The 100 kV high voltage platform is operational and the first section of the low energy beam transfer line (LEBT) necessary for the beam analysis and characterization has been assembled. The LEBT line (shown in FIG. 5) consists of a solenoid to provide the necessary beam focusing, a four sector ring to measure beam misalignments and inhomogeneity, a second current transformer to measure the beam current and a 10 kW beam stop.

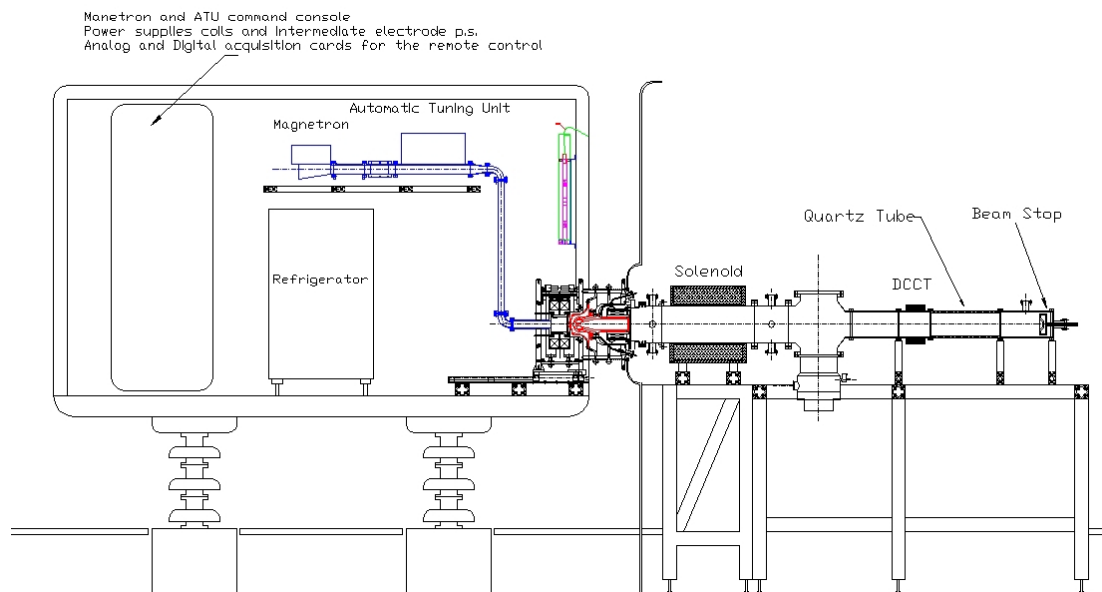


FIG. 5: The LEBT layout

The microwave injection system and the ancillary equipment (power supplies, MW generator, etc.) have been tested and installed. In particular: the microwave coupling with the matching transformer and the tuning unit works fine permitting to have very low values of reflected power. The first plasma has been obtained for the coils parameters (positions and currents) close to the calculated ones and the moving solenoids permit to optimize the ionization process by trying different magnetic field profiles.

A first beam of 20 mA at 50 keV has been produced by the source at very low RF power (220 W).

Some failures induced by HV sparks stopped these first promising operations. Different modifications are under way not only to solve this problem, which is common in this type of sources, but also in order to obtain the long-term reliability requested by the ADS facility.

Finally, an interceptive beam emittance measurement station from the CEA/Saclay, used at the SILHI source, will be moved to LNS for the beam characterization. FIG. 6 shows the TRIPS source and the LEBT installed at LNS in Catania.

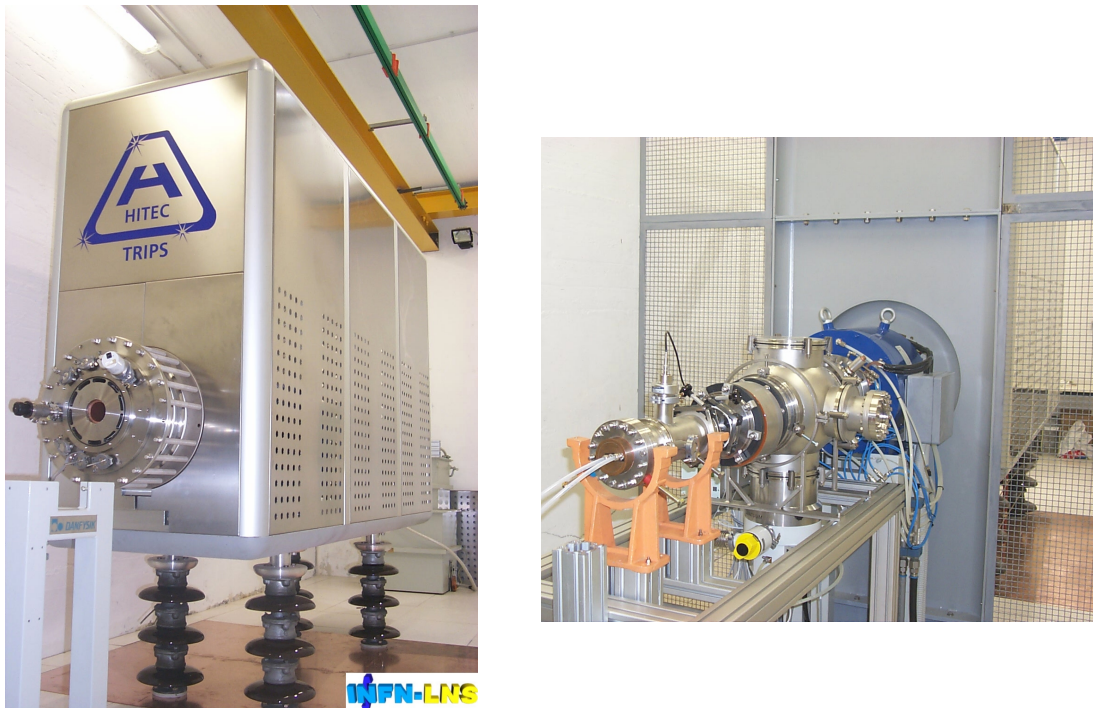


FIG. 6: The TRIPS high voltage platform (left) and the first section of the LEBT line.

2.5 Data validation

Many measurements at the CEA source SILHI have been taken in order to verify that the TRIPS source will be able to fulfill the TRASCO requirements. The SILHI source has been run at 80 kV, yielding a 77 mA proton beam with a beam emittance of 0.17π mm mrad (FIG. 7), thus providing a current twice higher than the one needed for TRASCO, at the same beam emittance.

These low emittance value has been obtained by controlling the injection of Ar in the LEBT line, with a pressure of $4.6 \cdot 10^{-5}$ Torr. A more general study of the dependence of the emittance from the gas pressure in the LEBT has been done ^{6,7)} (FIG. 8).

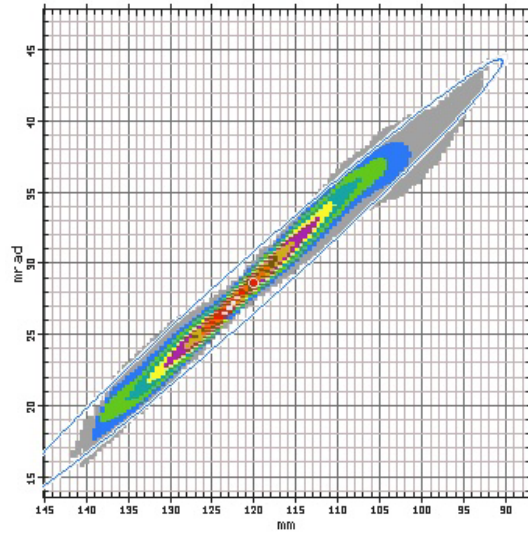


FIG. 7: SILHI measured emittance at 80 keV for a 77 mA proton beam.

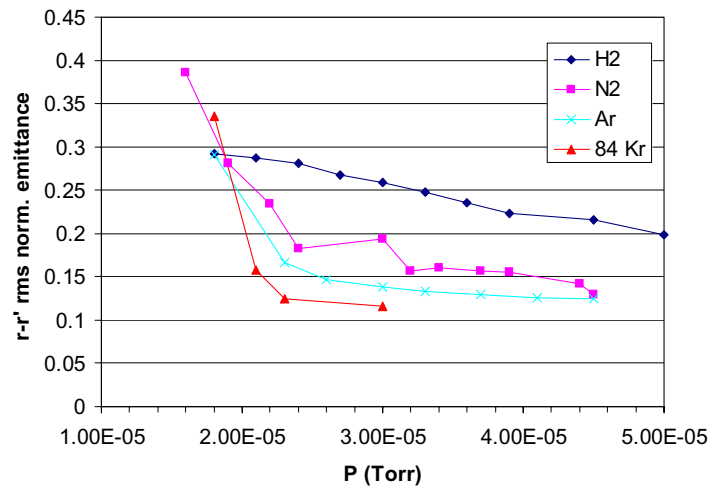


FIG. 8: RMS normalized emittance vs. beam line pressure for a proton beam of 75 mA.

We have also investigated the more stringent request concerning the reliability with a 12 hours test with the SILHI source working in conditions similar to the ones that will be used by TRIPS (TAB. 1).

The beam availability obtained during this period is 99.72 %. During this test only one spark occurs after 80 min. of operations: the extraction and puller power supplies fell down. The beam has been recovered within 2 min. after resetting the computer located on the high voltage platform. In FIG. 9 the beam energy and the beam intensity vs. the elapsed time are shown.

TAB. 1: SILHI Settings during the one day reliability test.

Parameter	Value	Units
Extraction voltage	80	kV
Puller voltage	40	kV
Screening electrode voltage	-2.8	kV
Discharge power	500	W
Beam current	75	mA
LEBT Pressure	$1.8 \cdot 10^{-5}$	Torr

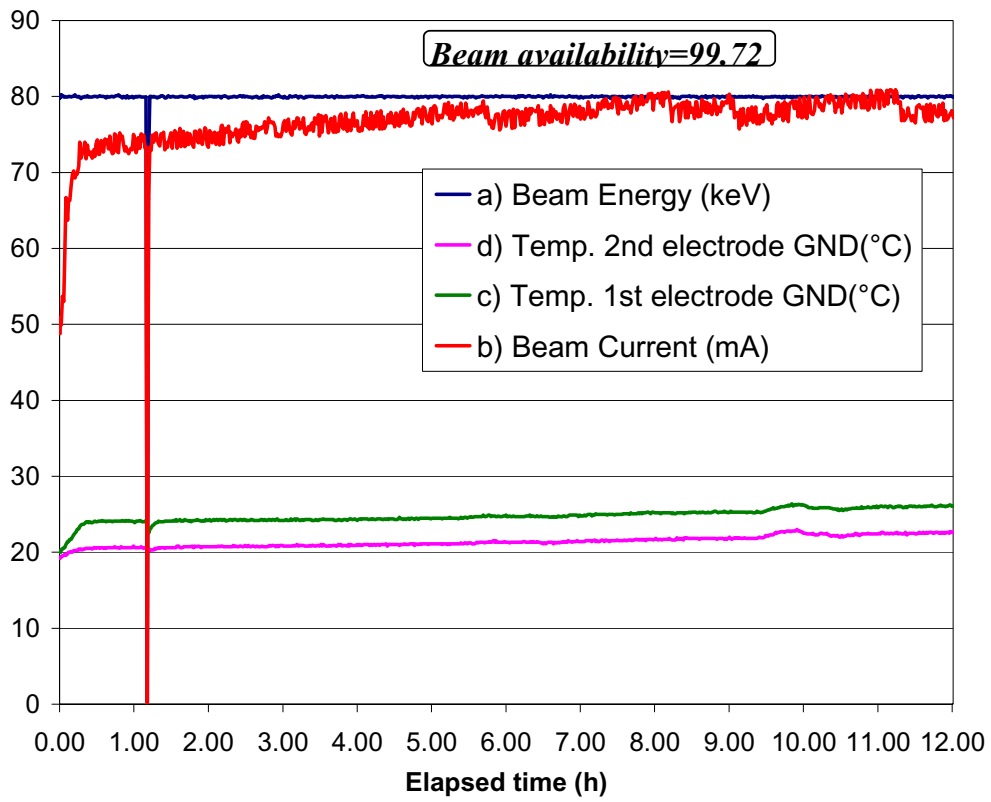


FIG. 9: Source parameters vs. elapsed time during the 12 hours test.

3 THE LOW ENERGY SECTION

The low energy linac, following the microwave discharge ion source, in our nominal design is composed by an RFQ and a superconducting linac (ISCL) (FIG. 10)¹⁷⁾; at low energy the beam is more sensitive to space charge and in general to perturbations, so that the design and construction of this part of the linac is particularly demanding. Our design choice has been driven by the requirements of reliability (continuity in beam delivery to the subcritical assembly), power conversion efficiency and compactness. The prototypes under construction at LNL are the first third of the RFQ and one of the superconducting cavities, of reentrant-type. As an alternative the option of a normal conducting DTL up to 100 MeV has been considered in detail.

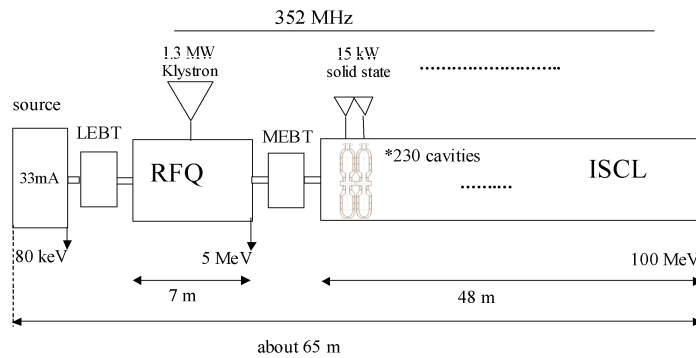


FIG. 10: Block diagram of the low energy section of the linac.

3.1 The TRASCO RFQ

In TAB. 2 the main RFQ parameters are listed²²⁻²⁴⁾. In particular the beam loading is less than one fourth of LEDA, the 100 mA, 6.7 MeV RFQ commissioned at Los Alamos National Laboratory⁵⁶⁾, which is necessarily a point of comparison. The lower beam power makes possible (and necessary) a different optimization of the design. For example, we can use a single klystron and keep a lower power dissipation density in the cavity. The TRASCO 352.2 MHz RFQ has been designed to accelerate relatively high current proton beams (30 mA) with beam losses lower than 4%, to prevent copper activation.

The main design constraints are determined by the maximum surface electric field, which has been set to 33 MV/m, i.e. 1.8 times the Kilpatrick value at the frequency of 352.2 MHz, and the available RF power, that we set assuming the use of a single LEP type klystron with a nominal power of 1.3 MW.

In FIG. 11 we show the schematic layout of the four vane RFQ, mechanically divided in six sections, flanged together. The position of the vacuum ports, slag tuners, RF couplers and other details are indicated.

TAB. 2: RFQ Design Parameter

Parameter	Value	Units
RF Frequency	352.2	MHz
Initial Energy	80	keV
Final Energy	5	MeV
Proton Design Current	30	MA
Duty factor	100	%
Maximum Surface Field	33	MV/m
Kilpatrick Factor	1.8	
rms Design Transverse Emittance	0.2	π mm mrad (norm)
rms Design Longitudinal Emittance	0.18	π deg MeV
RFQ Length	7.13	M (8.4 λ)
Intervane Voltage	68	kV
Transmission @ design current	96	%
Modulation	1-1.94	
Average Aperture R_0	2.9-3.2	mm
Synchronous Phase	From -90 to -29	deg
Q factor (SF/1.2)	8261	
Dissipated Power (SF*1.2)	0.579	MW
Beam Loading	0.1476	MW
RF Total Power Consumption	0.726	MW

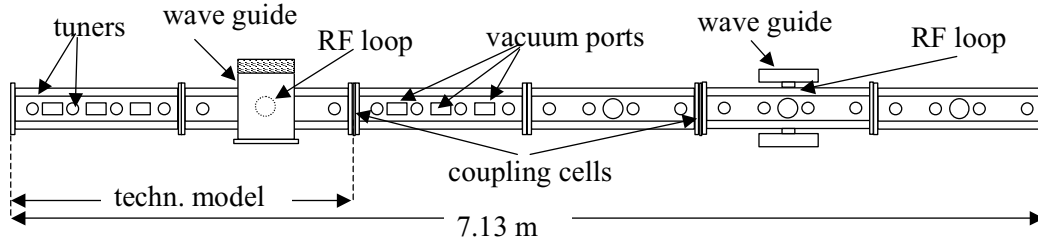


FIG. 11: Schematic layout of the TRASCO RFQ.

3.1.1 The RFQ design and beam dynamics studies

The RFQ has been designed with the four traditional sections: the radial matching section, the shaper, the gentle buncher and the accelerator. The focusing factor B is rather high, so to allow a robust dynamics against non-linearities due to space charge and vane geometry generated multipoles. In this last section, that is nearly 75% of the total structure length, the voltage is kept constant, while the average aperture is increased to allow a higher electrode modulation; the required minimal aperture and beam acceptance is kept.

This choice allows some saving in RFQ length even without any voltage ramping, and consequent increase of the dissipated power density.

These design choices have been extensively simulated using the code PARMTEQM of LANL ⁵⁷⁾, and crosschecks for the nominal design have been done with two other codes (LIDOS.RFQ of Bondarev and TOUTATIS of CEA/Saclay ⁵⁸⁾). All three codes predict a beam transmission in excess of 96% for beam currents up to 50 mA, with losses mainly located below 2 MeV. The total power deposited on the structure is approximately 1 kW, with only 210 W at energies above 2 MeV.

FIG. 12 shows the longitudinal variation along the RFQ sections of the average aperture R_0 , the beam aperture a , the focusing parameter B , the modulation factor m , the acceleration factor A , the surface field E_s , and the synchronous energy (W_s) and phase (ϕ_s). show the resulting beam dynamics simulations.

A 50 mA proton beam has been simulated under various conditions, so to test the tolerances to errors; in all cases we evaluate the beam transmission and the final longitudinal emittance, that are both sensitive design parameters. As an example a mismatch lower then 6%, a beam misalignment better then 0.25 mm and a source rms. normalized emittance better then 0.23π mm mrad are required. These figures are consistent with the source and LEBT specifications.

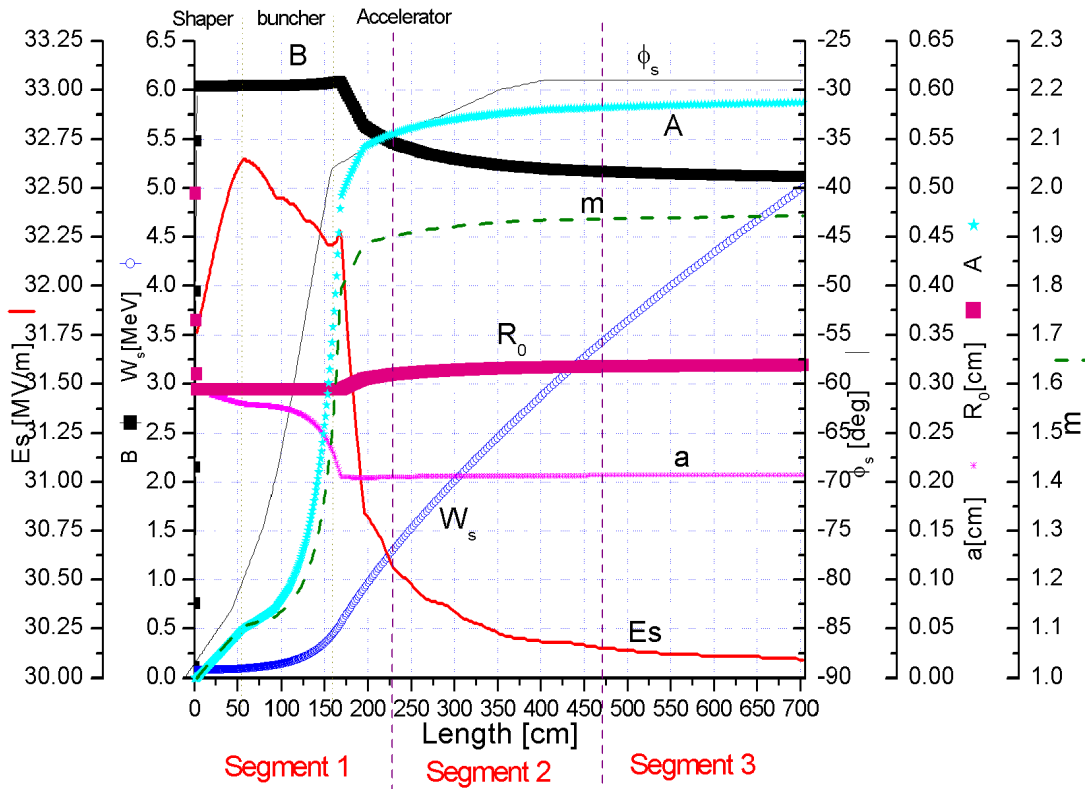


FIG. 12: Longitudinal variation of the RFQ design parameters along the three sections.

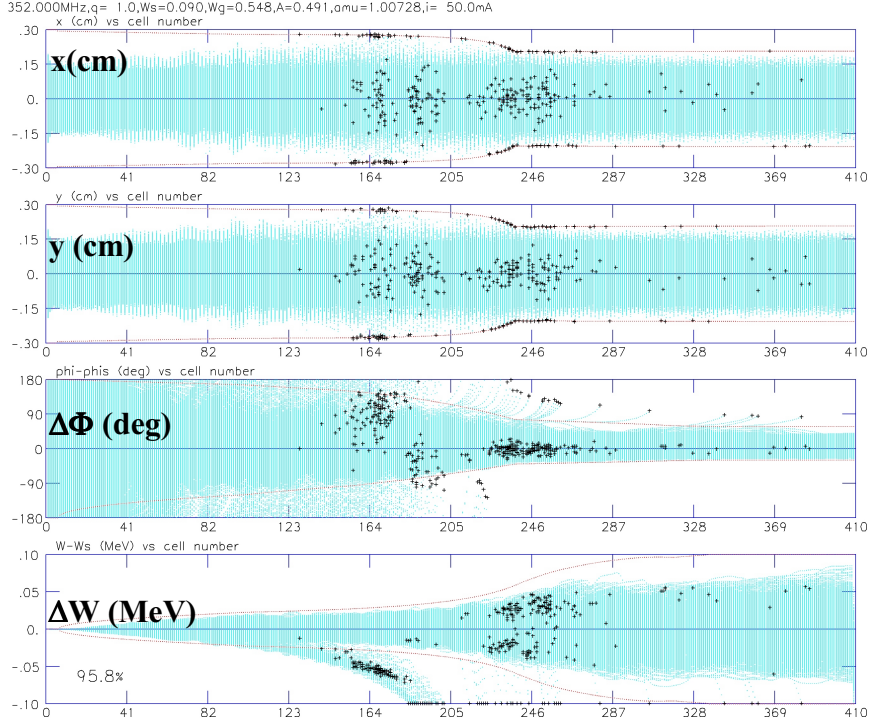


FIG. 13: Macroparticle coordinates as a function of cell number.

A field homogeneity error study allowed setting the tolerance of $\Delta E/E$ approximately to $\pm 1\%$, in order to maintain the nominal beam transmission. This requirement sets the maximum local frequency variation to approximately 40 kHz that is compatible with our mechanical tolerances and field adjustment procedure.

3.1.2 Electromagnetic and thermal analysis of the RFQ

The structure has a length of 7.13 m, equal to 8.4 times the RF wavelength in vacuum. This makes difficult the achievement of a flat voltage, since the spurious modes are close to the operating mode and a small error in the local cut-off frequency can generate a relevant field tilt. For a continuous four vanes RFQ with our length and frequency the first quadrupole mode was 0.6 MHz distant, so that a 6 kHz error in the local cut-off frequency would be enough to spoil the field distribution.

We therefore divided the structure in three resonantly coupled segments, following the LANL technique^{19,20,21,59}. The operating mode is about 2 MHz distant with respect to the closest quadrupole modes and the dipole modes are outside the range of the main quadrupole band. Each segment will be built in two longitudinal sections and each section is a sandwich of four parts, built in OFE copper, brazed together in a vacuum furnace. Four coupler ports, one in each quadrant and at two longitudinal positions, will feed the RF power. A schematic layout of the RFQ is shown in FIG. 11.

The RFQ vane tips will be modulated with a high precision milling machine before the brazing; a single tool will be used, with a transverse radius of 2.93 mm. As the average aperture increases in the accelerator section, the RFQ voltage is kept constant and the cut-off frequency is maintained by increasing the transverse section dimensions (to provide a change to the RFQ inductance as the capacitance varies by increasing the average aperture).

The electromagnetic design has been carried out using 2D Superfish (SF) and 3D (MAFIA) computer simulations. While 2D simulations have been used to determine the basic design and to evaluate power dissipation and frequency shifts due to boundary deformations, the 3D simulations have been used to model the intrinsically 3D details (end-cells, coupling cells, tuners, vacuum port grids, etc..., as shown in FIG. 14). Few global runs were made to compare the RF field distribution with transmission line calculations and to bead pull measurements on the aluminum model.

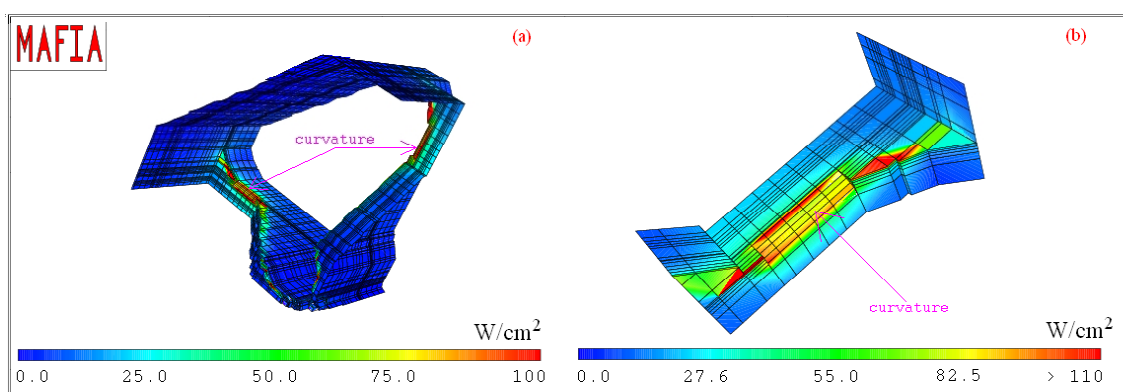


FIG. 14: Power dissipation at electrode terminations (MAFIA).

The thermal behavior of the RFQ cross section has been analyzed using the codes ANSYS and SF. The RF power source used is 1.5 times the SF distribution, for a total of about 1 kW per structure cm: 20% margin is due to the lower Q of the real structure, while the possibility to work with 10% higher voltage is kept open.

The mechanical deformation, calculated by ANSYS for the given cooling channels distribution, determines the (local) frequency shift by means of Slater theorem. The heat exchange between water and copper is calculated for the given water velocity (< 4 m/s as a design parameter) and channel shape.

The goal is to keep below 20 kHz (threshold for acceptable field variation) the local frequency shift between RF on and RF off, and between the beginning and the end of a 1.2 m section (water input and output). The first requirement guarantees that the tuners position, determined at low RF level, is still valid in operation; the second avoids field bumps due to the water temperature rise along the channels.

In FIG. 15 we plot the temperature maps and the deformation maps at the beginning (left) and at the end (right) of one RFQ section; both the requirements have been fulfilled. The total water flux is of about 3000 liters per minute.

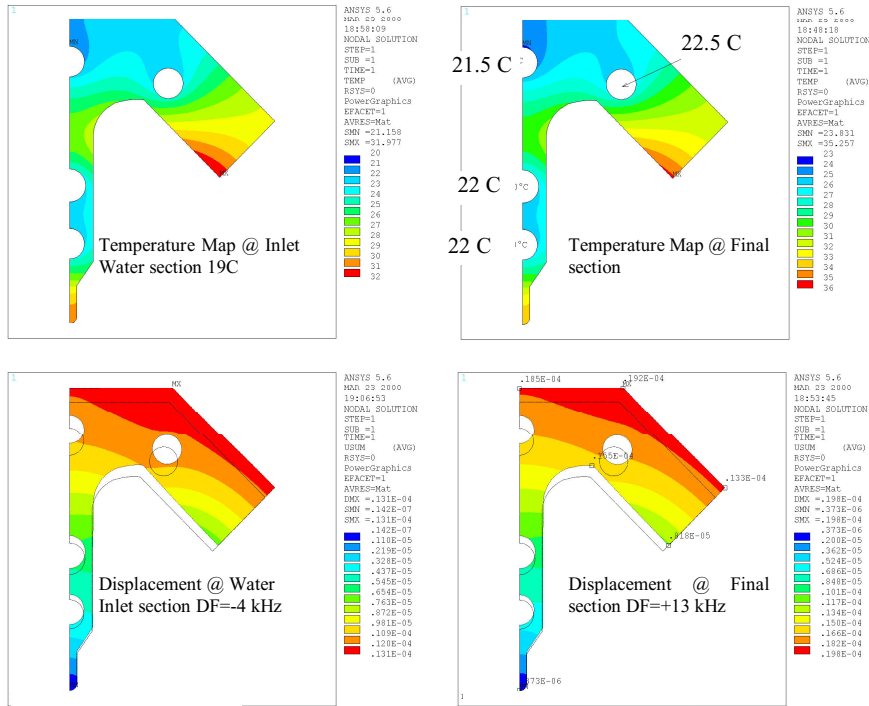


FIG. 15: Temperature field (top) and induced deformations (bottom) at two longitudinal positions along one RFQ section (beginning and end of the cooling water channel)

The mechanical construction errors will be much larger than the thermal deformations, so that a correction system to be used a posteriori, (i.e. after the brazing), is needed. Typically a 20 μm error in the vane tip position corresponds to 1 MHz error in the local frequency. For this reason the RFQ is provided with 96 tuners, with a ± 1.5 MHz tuning range; the technique to make flat the field using the tuners in such long and resonantly coupled RFQ is not trivial, and has required the construction of a 3 m long aluminum model where many RF measurements have been performed and the field stabilization demonstrated (FIG. 16).

3.1.3 The technological model

As part of the TRASCO program, the first segment (indicated in FIG. 11) is being manufactured by the Italian company CINEL and will be tested at CERN with full power. The two remaining segments will be built in an extension of this program.

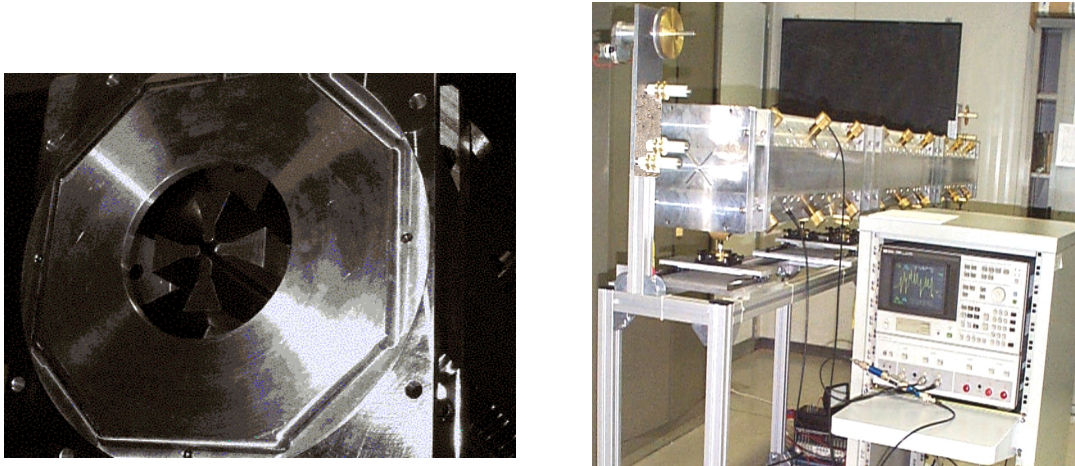


FIG. 16: Aluminum RFQ model built for low power RF tests.

The first segment, meant as a technological model, allows checking the construction of all the main components, as well as the tuning procedure and the high power behavior. Construction details like the deep-drilled channels, the brazing procedure, the vacuum ports with cooled grids, the tuners with pick up loops and the feeder loops, will all be checked in the most realistic conditions (except for beam).

A first piece of structure, 220 mm long, but able to test the main construction difficulties, is being milled now (FIG. 17).



FIG. 17: Test of the RFQ construction
(the four parts after thermal treatment and before final machining).

In particular each of the four coupling loops need to deliver about 180 kW of RF power to the structure. A similar solution to that used for the normal-conducting LEP cavities has been designed, even if the power is somewhat higher than demonstrated with the LEP windows⁶⁰). The coupler geometry, and in particular the wave guide to coaxial transition and the RF drive loop has been extensively studied with HFSS and optimized for maximal transmission and critical coupling. The high power RF tests at CERN will be used to verify the RFQ structure Q and the power coupler performances.

3.2 The reference DTL design

The possibility to use a room temperature linac up to approximately 100 MeV with the conventional configuration of a proton source feeding a RFQ followed by a DTL has been initially considered for TRASCO¹⁴⁾. The idea behind this choice is that the superconducting linac has the biggest impact on both capital and operational costs and most of the technologies exist at present. The injector instead has a relatively smaller economical impact and it is surely worth considering a design based on a conservative, and “standard”, option.

A three section DTL, with transition energies at 20 and 70 MeV has been investigated, at the 352.2 MHz LEP frequency. In each section the quadrupole magnets are identical and geometrical parameters of the RF cavities as the diameter and the beam bore radius are kept constant. The whole linac length is approximately 80 m.

An important figure of merit of a DTL is the shunt impedance, which should be high as possible to limit the dissipated power on the structure. An efficient DTL, with high shunt impedance structures, ask for small drift tubes, which unfortunately need to house the focusing quadrupoles.

The focusing structure is a $2\beta\lambda$ lattice with a transverse phase advance of 25° , provided by an electromagnetic quadrupole integrated strength of 2 T. Since the drift tube length increases with β , the three families of quadrupoles have increasing length and decreasing gradient. Moreover, since at high energies the quadrupole design is less critical, the bore radius can be increased leaving more margins for the beam.

From the constructive point of view the DTL proposed is a standard structure suitable to stand the CW operation. The quadrupoles magnets, housed in the drift tubes, are made in soft iron with high saturation field, with hollow conductors for water-cooling (4 by 3 mm with a 2 mm hole). The drift tubes are realized in bulk copper with an adequate cooling circuit. The dimensions of the tubes are dictated by the quadrupole magnets and by the thickness of the copper wall that has to be large enough to efficiently transmit the heat generated by the RF dissipation to the cooling circuit. The drift tube dimensions and shape are critical for obtaining a high shunt impedance.

The RF field distribution, the geometries to reach the proper resonant frequency and the structure efficiency have been computed using SUPERFISH code for the generation of the cells at different energies. At every transition between the DTL segments the tank diameter is reduced, so that the gap length can be decreased keeping the resonant frequency and more space for longer quadrupoles is available. The beam dynamics has been simulated with PARMILA code and the DTL aperture is always between 8 and 12 times the beam rms radius, a safe value at these energies.

Due to the low shunt impedance value of the RF structures a 100 MeV, 30 mA linac dissipates approximately 9 MW in the structure, a considerable amount of power that, at these moderate currents, has a non-negligible impact on the whole linac efficiency.

3.3 The superconducting ISCL

A superconducting option for the 5-100 MeV linac is under study for TRASCO. We considered an Independently phased Superconducting Cavity Linac (ISCL) similar to those used for low energy heavy ions in many nuclear physics laboratories like ours, but at much higher beam intensity, and in a wider beta range ¹⁵⁾. We checked various kind of cavities and we selected the so-called “reentrant cavities”, that are modified pillbox, cylindrically symmetric and therefore theoretically dipole free. ¹⁷⁾

One of the advantages of this kind of linac is its remarkable flexibility, that allows using it CW at lower current or even with different kind of particles, like deuterons. In TAB. 3 we list the main specifications and machine characteristics. In particular we specified the two main constraints of the independently phased resonators: the surface field and the beam loading per cavity. The second constraint is specific of high current machines: in our case we want to feed each cavity with a single solid state amplifier and the limitation to 15 kW is consistent with the present technology.

TAB. 3: ISCL Design Parameters

Parameter		Value	Units
Energy range		5-100	MeV
Total length		48	m
Synchronous phase		-40	deg
Average acceleration		1.82	MeV/m
Number of cavities		230	
Cavity bore radius		1.5	cm
Quadrupole gradient		31	T/m
Quad aperture/length		2/5	cm
Output	Trans. (normalized)	0.42	mm mrad
RMS Emittance	Long.	0.2	MeV deg
Current limit (losses 10^{-4})		>50	mA
RF dissipation ($R_s=100\text{ n}\Omega$, $R_{BCS}=58\text{ n}\Omega$)		1204	W(@4.5 K)
Beam loading		2.85	MW
RF sys. pwr. cons. ($\eta_{RF}=50\%$)		5.7	MW
Static cryogenic losses (10 W/m)		480	W
Cryogenic Consumption ($\eta_{cryo}=1/500$)		0.84	MW
Quadrupoles and ancillaries		0.5	MW
Mains power		7.04	MW
Power conversion efficiency		40%	

An additional constraint is given by the reliability requirements typical of an ADS, where the operation with a sub-critical reactor is spoiled even by a beam shut down of a second. To meet these requirements we have chosen an architecture with reliable solid

state amplifiers. Even in the presence of a large number of such RF systems with finite reliability, we required that the beam could be transmitted in case of failure of a cavity. This is connected to the requirement that the acceleration per cavity plus the energy spread is smaller than the separatrix energy width. If the beam survives the failure of a single amplifier, and the amplifier is replaced on line, the resulting availability of the linac is highly improved.

We have chosen a FODO focusing structure with period $8\beta\lambda$. As the period becomes longer, a larger number of cavities can be installed between the quadrupoles (FIG. 18).

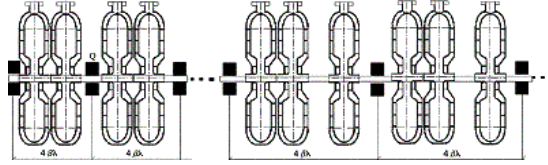


FIG. 18: ISCL lay out: reentrant cavities and quadrupoles in the cryostat.

The required gradient can be reached both by normal conducting and superconducting quadrupoles. Nevertheless, due to the lack of space, it is necessary to use superconducting quadrupoles installed inside the same cavity cryostat.

3.3.1 The reentrant cavity design

The cavity geometry has been analyzed with the SUPERFISH code, and the main parameters are reported in TAB. 4.¹⁸⁾ Since the performances of the reentrant cavities have been limited in the past by the strong multipacting behavior of the pillbox shape with a flattop equator, the cavity shape has been modified with an elliptical equator shape, in order to lower the field levels in the equatorial region.

Since the main limitation in low- β superconducting cavities is usually determined by the maximum achievable surface electric field, related to the onset of field emission, and since our linac design required relatively low energy gain per cavity, we looked mainly for low surface electric and magnetic field, and short physical dimensions.

The RF power will be fed through a inductive coupler, still under study, located on the resonator equator. A deep study of the multipacting (MP) properties of the cavity was performed, with more than 50000 runs of the simulation program TWTRAJ. The region where most of the multipacting levels is concentrated, in the “pillbox” design, is the resonator equator. Electrons originating in high electric field regions drift to the equator and are collected there, building very strong levels with various multiplicities. This region has been properly shaped with an elliptical contour (ratio between axes 1:1.5) and all high field levels have been finally eliminated. The results can be seen from FIG. 19.

TAB. 4: Resonator parameters calculated by means of the code SUPERFISH.

Parameter	Value	Units
Total length	135	mm
Internal length	80	mm
Bore radius	15	mm
Frequency	352.2	MHz
U/E_a^2	0.034	J/(MV/m) ²
E_p/E_a	3.05	
H_p/E_a	30.6	G/(MV/m)
$\Gamma=R_s \times Q$	83.9	Ω
R_{sh} (Cu)	18	M Ω /m
β	≥ 0.1	

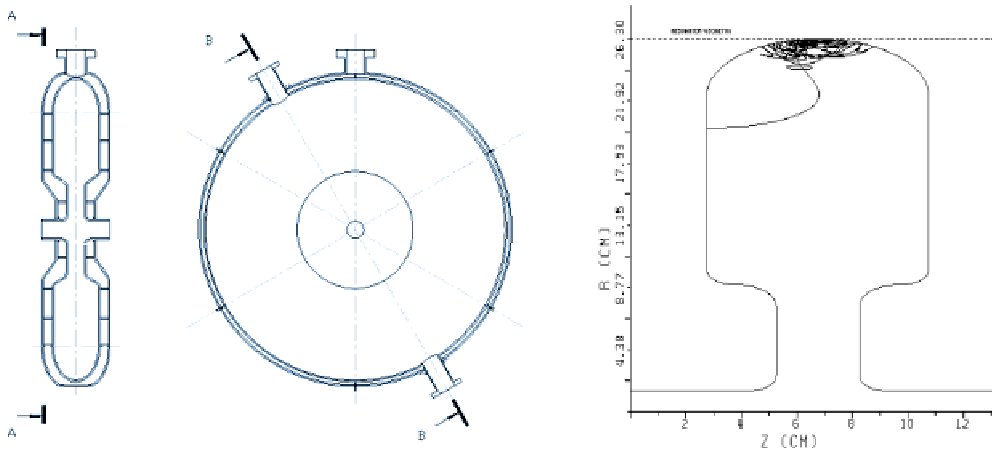


FIG. 19: The reentrant cavity mechanical design (left). Example of the multipacting simulation program output (the horizontal axis is stretched in the picture). The circular contour, as well as the rectangular one, was causing high field multipacting levels (right).

The main concern in the mechanical design was related to the large force acting on the relatively flat and wide resonator surface. The niobium sheet, 3 mm thick, could not sustain the pressure in the absence of strong reinforcement.

We tackled this problem using a different approach: in our design, the helium vessel is part of the resonator and is welded to the resonator wall so that the net force on the total structure is nearly cancelled. This design allows a relatively light structure with a good stability and a minimum displacement of the walls under pressure (limited to a few microns) when the tuner is mounted. The mechanical stresses are also confined to rather safe values. The 4.2 K helium is fed by gravity through a flange on the top of the resonator; like in most superconducting linacs for heavy ions, there is no separation between the beam vacuum and the cryostat one.

The tuning is obtained, changing the gap length, by means of a mechanical tuner connected to the external part of the drift tubes. A “nutcracker” type tuner, driven by a piezoelectric or magnetostrictive actuator, is being presently considered. Since the required tuning force is relatively low, the calculated Lorenz force detuning ($170 \text{ Hz}/(\text{MV}/\text{m})^2$) and helium pressure detuning ($140 \text{ Hz}/\text{mbar}$) of the bare cavity are not negligible in comparison to the 1 kHz resonator RF bandwidth in operation. A stiff tuner reduces the pressure detuning to $\sim 20 \text{ Hz}/\text{mbar}$. The foreseen CW mode of operation gives a nearly constant radiation pressure on the walls that can be compensated by the tuner. The experimental study of possible mechanical instabilities and of their remedies, however, is one of the aims of this prototype construction. For the design and simulation of the mechanical structure we used the I-DEAS code.

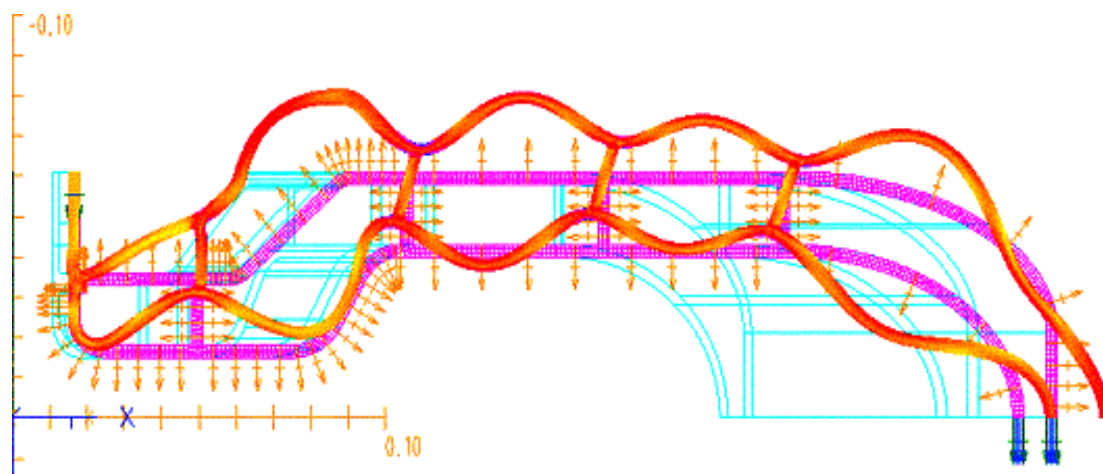


FIG. 20: Mechanical deformation as a result of 1 bar pressure increase in the helium bath. The maximum displacement is about $20 \mu\text{m}$ in the outer shell (for clarity, the deformation is amplified in the picture).

3.3.2 Development of high power, low cost solid state amplifiers

The 15 kW beam loading foreseen for the 352.2 MHz superconducting reentrant cavities can be provided by RF amplifiers based on the vacuum tube technology (tetrodes, klystrons, etc.) and also by solid-state devices. While the solid-state technology, below a few kilowatts, is anyhow preferable in terms of compactness, reliability and low cost, in the $10\div 20 \text{ kW}$ range the cost of commercial amplifiers (usually built for TV transmission) is generally higher for solid state devices than for vacuum tube ones. The main reason is that the maximum output power of solid state amplifying units hardly exceed 150 W, and a large number of such elements in parallel is required to reach high power. The amplifier cost, thus, is roughly proportional to its nominal output power. Above $10\div 20 \text{ kW}$, the vacuum tube technology is generally considered as the most convenient one.

A considerable cost saving, however, can be obtained by developing solid state 352.2 MHz RF amplifiers conceived for accelerator application (thus neglecting some of the TV transmission requirements) and based on high power MOSFET components. This activity is being pursued by INFN-LNL in collaboration with the French laboratory of LURE at Orsay ⁶¹⁾. Amplifying units of 300 W, each equipped by a circulator and a power supply to obtain a simple parallel assembly, have been constructed and successfully tested. One of the advantages of such scheme is that the failure of one unit would not stop the amplifier working but only reduce its maximum output power; this could be an important characteristic if maximum reliability is required.

3.3.3 Studies on 2-gap superconducting low beta cavities

The ISCL design based on reentrant cavities is justified by the constraint of a 0.5 MeV maximum energy gain per cavity; this value is dictated by the requirement of a beam transport without losses, with no change of the linac operational parameters, even in case of failure of one cavity. If this requirement can be fulfilled by means of a different method, a cost effective linac design could be based on 2 gap, high gradient superconducting cavities. The number of resonators would be nearly halved; the linac overall length and cost could be reduced significantly.

The experience acquired by INFN in the development of superconducting quarter wave resonators (QWR) for low beta heavy ions allow to aim to short cavities able to provide from 1 to 1.5 MeV acceleration ^{62,63)}. The beam loading per cavity would reach 30-45 kW, value that would allow the use of the CERN LEP RF couplers technology. This power range is very well covered by commercial klystrode RF amplifiers, that combine a very high efficiency, high gain and good linearity characteristics.

The field distribution in the RF gap of a short QWR contains a dipole component which could cause beam emittance degradation. Studies are being performed in order to minimize this effect, both by geometrical optimization of the cavity shape and by a properly designed linac lattice. The dipole field components are absent in Half-Wave Resonators (HWR), at the price of a more complicated geometry. HWRs performance is expected to be comparable or even superior to QWRs one.

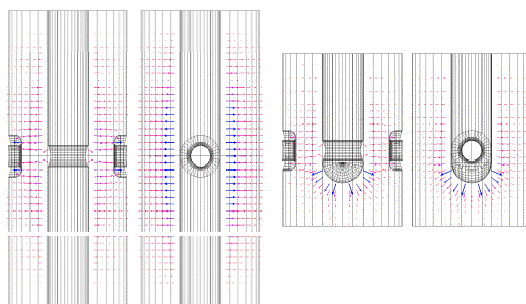


FIG. 21: HFSS simulation of $\beta=0.25$, 352 MHz Half- and Quarter-Wave Resonators.

3.4 Beam halo formation studies.

A specific research activity has been devoted to the investigation of the beam halo formation process. This is a crucial problem for the feasibility of a high intensity linac since even a very low relative loss of protons can lead to an intolerable activation of the structure, making unpractical and costly, if not impossible, the operation of the facility.

The maximum losses allowed in a proton accelerator (above 20-30 MeV) can be evaluated in 1-2 W/m, corresponding to 10^{-6} /m relative losses in the ISCL, and 10^{-7} /m at the end of the linac. These losses are associated with the presence very few particles at large distance from the average beam dimension (beam halo). It is generally recognized that the main mechanism that generates beam halo is due to the non-linear particle resonances driven by the space charge. In particular the resonances between envelope modes and single particle frequencies, which are excited in a mismatched beam, are one of the main causes of the space charge induced halo.

The usual approach to the problem is based on multiparticle programs and particle core model (PCM). In the first case one solves the self-consistent problem of the evolution of the whole particle distribution, but the number of particles is limited by computer capabilities. In the second case one simulates of the dynamics of test particles in the presence of a given particle distribution; in this way the diffusion of few particles, which does not affect the beam core, can be studied.

We have considered both directions by developing a 3D particle in cell program to solve the Poisson-Vlasov equation and a 3D PCM where the phase space analysis is performed using the frequency map technique.

The PIC code is based on a symplectic tracking of each macroparticle and a fast Fourier transform to compute the electric field of the distribution ²⁸⁾. The algorithms are suitable to be implemented in parallel computing architecture, so that during 2001 we shall be able to pass from the present 10^5 macroparticles to 10^6 - 10^7 , using a PC cluster. We have shown how an initial 3D Neuffer KV distribution relaxes towards a Fermi-Dirac distribution in few periods of a FODO channel, with RF gaps. The parameters correspond to the ISCL at 50 MeV (phase advance per period 84 deg transverse and 81 deg longitudinal, tune depression of 60%). In spite of this relaxation the macroscopic field of the distribution in any case is very similar to that of a uniformly charged ellipsoid.

Then we have considered a PCM, with the analytically calculated field of a uniformly charged ellipsoid ^{25,26,27)}. An effective representation of phase space both in the matched and mismatched beam case can be done using the Frequency Map Analysis, which associate to each trajectory the corresponding single particle frequencies.

Regular trajectories define a regular mapping between initial conditions and the frequency space, and a uniform grid of points in a given section of phase space should appear smoothly deformed in the frequency space; resonant trajectories correspond to

resonant frequencies that concentrate on the resonant plane. The amplitude of the resonant regions is proportional to the empty channel around the resonant plane.

In FIG. 22 we show the FMA in the transverse coordinate plane for a matched beam (left) and 10% mismatched beam (right). The lower part shows the regular grid of initial conditions while in upper part the corresponding frequencies are plotted. The straight lines in the frequency plot indicate the main low order resonances and the corresponding resonant initial conditions are plotted with different marks and different colors.

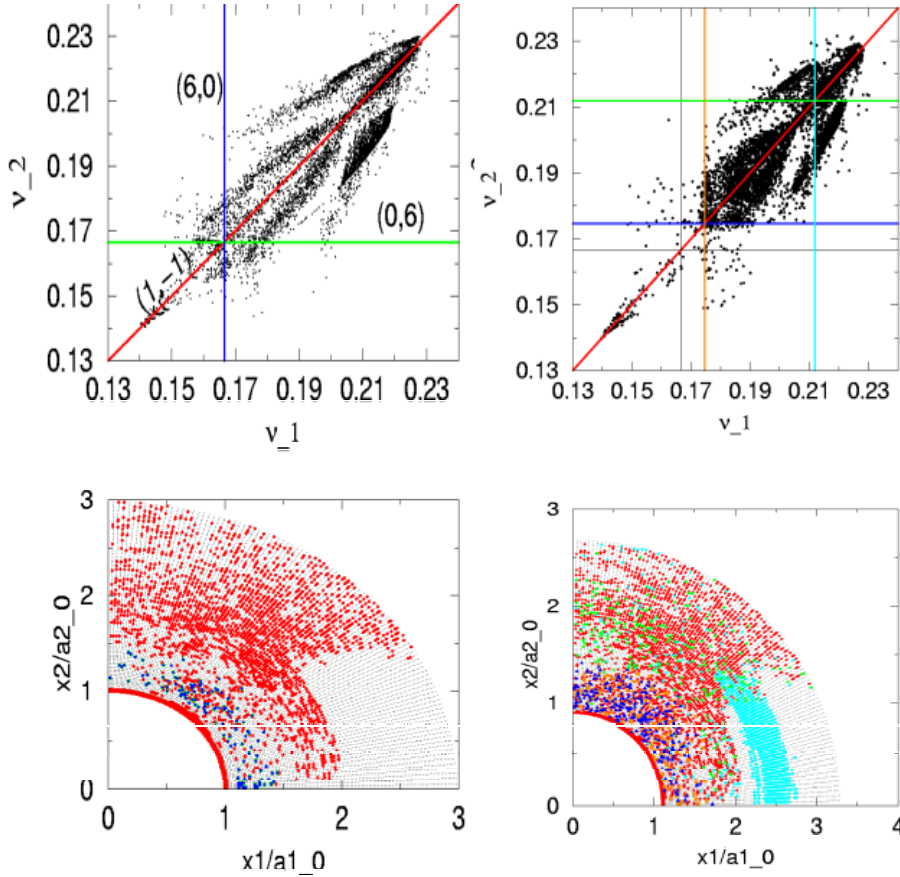


FIG. 22: FMA analysis of a matched (left) and a 10% mismatched beam (right).

The effect of resonances between the single particles tunes and the envelope modes can be clearly recognized in the frequency plots (horizontal and vertical straight lines) and their overlap with the $v_1=v_2$ shown in the plots of the initial conditions, creates a chaotic region where the orbits can diffuse up to large amplitudes.

This is confirmed by the direct tracking of $5 \cdot 10^4$ particles, chosen in a small annulus just outside the beam core (FIG. 23).

In the next year the FMA and the 3D PIC program will be integrated in a linac design code, able to study both the emittance exchanges and the low probability particle diffusion.

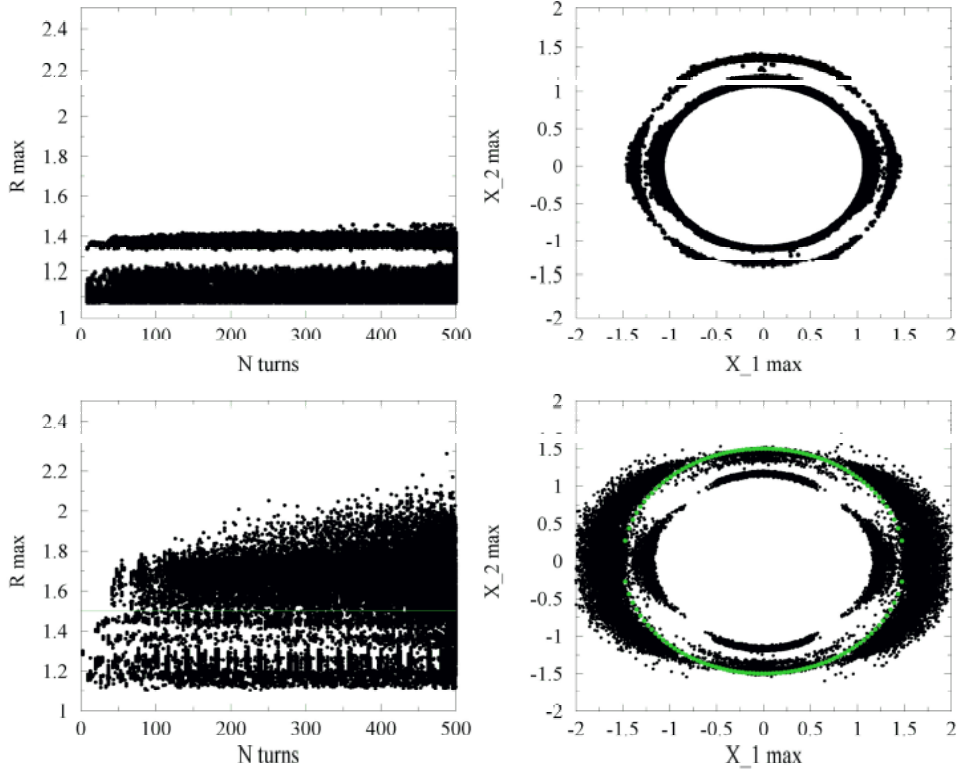


FIG. 23: Particle tracking for the same case as the previous figure.

Recently, a very fast damping of beam envelope oscillation amplitudes has been observed in simulations of very high intensity beams transportation (initial Gaussian distribution for $\sigma/\sigma_0=0.29$)⁶⁴.

Several simulations, with the modified multiparticle code PARMT, have been carried out, to point out in which conditions this fast damping occurs and what kind of mechanism could be responsible for it. The explanation found involves the so called Landau damping, i.e. the attenuation of coherent oscillations when the single particle frequencies have a spread.

In the simulation results of FIG. 24, it is shown a case in which the odd envelope oscillation mode quickly damps while the even one practically has no damping effect. In this simulation, we have used a mismatch of 10% on the beam size, the resulting odd rms envelope oscillation has a frequency of $\omega_o=64$ MHz, while the even mode frequency, ω_e , is 84 MHz. Only for the odd mode $\omega_o/2$ lies inside the beam betatron frequency distribution, centered at 20 MHz with a spread of 6 MHz. In the simulations shown, we have a coherent excitation, given by the breathing mode oscillation of the beam envelope and a large set of oscillators, the beam particles, oscillating with a large betatron frequency spectrum. Then, being satisfied, for the odd mode, the conditions required by the Landau damping mechanism, it will occur as confirmed by the results of FIG. 24. In the same figure, for the even mode, no damping is observed.

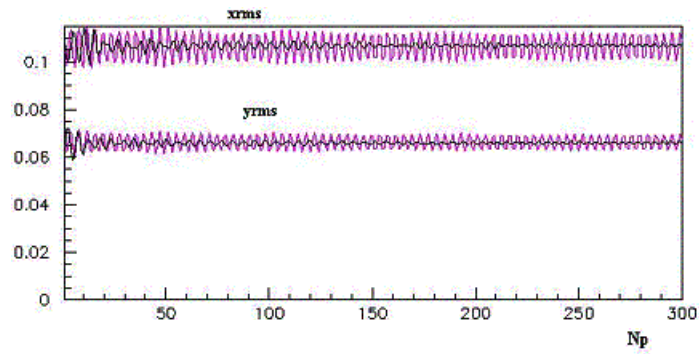


FIG. 24: The rms envelope oscillations with initial Gaussian distribution for $\sigma/\sigma_0=0.29$. The black line represents the odd mode, the magenta line the even mode.

This mechanism can be relevant for beam halo formation since halo particles appear mainly in the even oscillation case, in which beam envelope oscillations survive for a longer time.

4 THE SUPERCONDUCTING HIGH ENERGY LINAC

The starting energy of the high-energy superconducting linac has been set in the 90-100 MeV energy range. At energies below this range the decrease in length of the elliptical cavities, and the corresponding decrease in overall performances, favors the choice of either a standard normal conducting accelerating structure or the use of different resonant structure geometries, as discussed in the previous paragraph.

4.1 Choice of the frequency

The original choice of the 352.2 MHz frequency²⁹⁾ was motivated by a scenario in which a demonstrator ADS facility was decided to be built as soon as possible (as initially proposed by C. Rubbia for the EA/ADS demonstrator⁴⁾). At this frequency, in fact, all the required technologies have been proven by the CERN LEP experience, and most of the ancillaries exist with specifications close to the ADS requirements⁶⁵⁾ (couplers, tuners, cryostats, low level RF components, high power klystrons are good examples). The only point that needed an experimental demonstration was the feasibility of sputtered (Nb on Cu) cavities at low β values.

During the last two years it became clear that the envisaged time scale needed for an ADS demonstration plant will be longer than initially expected, and the bulk niobium superconducting RF technology set by the TESLA/TTF International Collaboration⁶⁶⁾ allows the design of better performing cavities with respect to the CERN sputtered technology, that dates back more than a decade.

As an example, the last 20 nine cell cavities built by the industries for the TTF operated with peak magnetic fields in the range between 80 and 100 mT before the Q dropped below the 10^{10} value⁶⁷⁾, while the standard sputtered cavities operation is limited to 35 mT, with a Q greater than 2×10^9 . Moreover, the R&D activities carried out for TRASCO and those undergoing at CERN have proven that the sputtered technology can be adapted to moderately low- β cavities⁵²⁾ (down to the 0.7 range), but the tests with low β cavities (around 0.5) consistently gave unacceptable Q-slopes even at moderately low accelerating fields, presumably explained by a bad Nb film growth due to the short cavity shape⁶⁸⁾.

Doubling the RF frequency to 704.4 MHz, and using the know-how gained by the TTF Collaboration for the development of the missing ancillary components at these frequencies, the superconducting linac length can be nearly halved, using the possibility of operating reliably at almost double accelerating gradients with bulk Nb cavities. The additional complication of operating at 2 K is overcome by this drastic reduction in linac length. One of the advantages of the 704.4 MHz frequency is that the cavities are 8 times smaller in volume with respect to the CERN cavities, and several infrastructures for cavity fabrication, treatment and measure exist (notably CEA/Saclay) or are being set up (as in

INFN Milano/LASA) in Europe. These smaller cavities also show a better mechanical stability (again related to the smaller physical dimensions). We may conclude this discussion on the frequency choice stating that the 352.2 MHz RF could be considered a valid choice if the energy required for the beam is high enough to take advantage of the “cheap” sputtering technique (above 1 GeV) and a demonstrator ADS needs to be built in a short time frame, in close collaboration with CERN and making use of its large infrastructures. Conversely, the 704.4 MHz choice leaves more space for making use of the technological improvements obtained in the past years by the TESLA/TFF International Collaboration, as it has been successfully proven by both the single cell $\beta=0.64$ cavities developed by CEA/Saclay and the single-cell $\beta=0.5$ cavity that we have built for TRASCO³⁹⁻⁴³.

4.2 Technological activities for the cavity production

On the basis of the motivations expressed in the previous paragraph, two parallel experimental activities have been followed in order to assess the feasibility of both frequency options. Two linac configurations, making use of general scaling laws of the linac design as a function of the frequency, have been determined and used for the cavity R&D activities. The first activity, in collaboration with CERN, aimed at reaching the same LEP cavity performances with a $\beta=0.85$ sputtered cavity, the other aimed at proving the reliability of the bulk Nb technology for the low $\beta=0.5$ cavities.

4.2.1 The Nb sputtered on Cu cavities built with CERN

One single cell and one five cell $\beta=0.85$ cavity have been built and tested by CERN with the TRASCO design at 352.2 MHz, with results exceeding the design specifications⁵²). The results for two series of tests of the five-cell cavity, before and after He processing, are shown in FIG. 25. The figure shows the cavity quality factor, Q , as a function of the accelerating field (E_{acc} , in MV/m). The upper horizontal axis shows the peak magnetic field on the surface (directly proportional to the E_{acc}). The ratio of the peak surface fields with respect to the accelerating field depends entirely on the cavity geometry and is higher for lower β cavities than for electron ($\beta=1$) cavities, like the LEP II cavities. Taking into account this fact the Q vs. B_{peak} curve of the TRASCO $\beta=0.85$ cavity measurement falls entirely in the production spread of the last LEP II cavities batch. The dashed area in the figure indicated the operating region of the cavities, with a design value of $Q=2 \times 10^9$ at the accelerating field of 6.5 MV/m.

An ongoing extension of the agreement with CERN will allow us to equip the cavity with a He tank, the standard LEP tuner, coupler and HOM, install it in a specially modified spare cryomodule, and test it in the LEP cryomodule test bench.

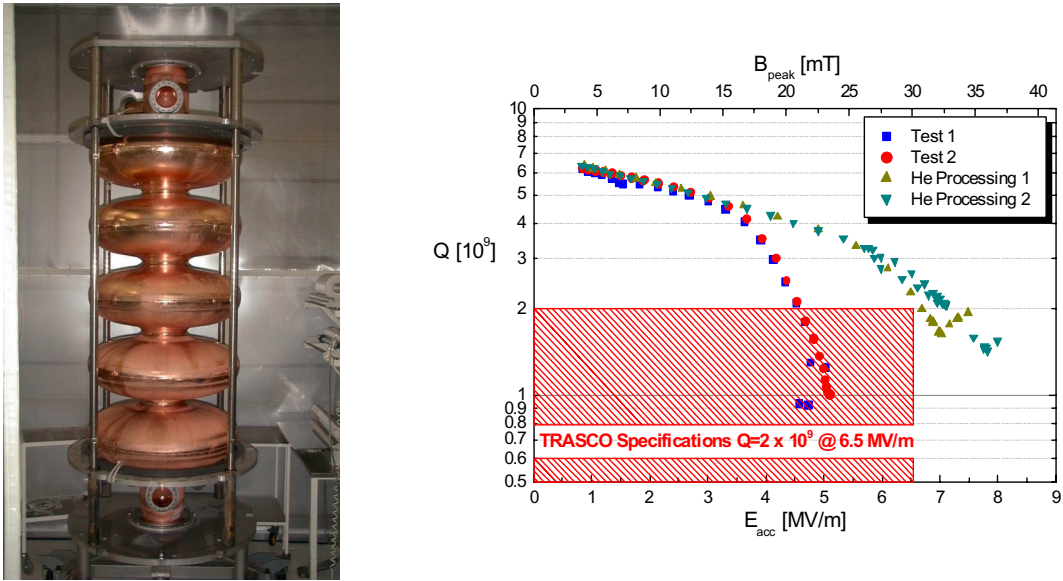


FIG. 25: Picture and Q vs. E_{acc} plot of the $\beta=0.85$ Nb/Cu five cell cavity tested at CERN.

4.2.2 The bulk Nb cavities

A single cell $\beta=0.5$ cavity has been manufactured by one of the TRASCO industrial partners (Zanon) using the low-grade (reactor grade, with minimal RRR=30) niobium sheets that we purchased mainly for the test of the deep drawing dies. After e-beam welding the cavity has been sent to CEA/Saclay for the chemical treatments and RF tests. Due to the low quality of the Nb sheets, the cavity was not expected to reach high fields. However, the tests at Saclay were very successful, and the cavity performed very well above the design specifications of a $Q=1 \times 10^{10}$ at the accelerating field of 8.5 MV/m, as shown from FIG. 26, where we also show pictures of the cavity during fabrication and test. Moreover, the Q factor does not exhibit any significant slope up to fields greater than the nominal operating field⁴³.

The residual resistivity ratio estimated from the RF measurements is RRR=58. After reaching an accelerating field value of 10.5 MV/m the cavity abruptly quenched. The cavity will be tested again both in Saclay and in Milano when the cavity test area will be operational, in late Spring 2001. The performance of this first $\beta=0.5$ cavity, especially when compared with the unsatisfactory results of the low beta sputtered cavities obtained at CERN due to the bad film quality, is extremely encouraging and Zanon is currently manufacturing three additional single cell cavities. One is being built with the low-grade niobium, while the last two are being built from high quality (RRR=250) sheets.

The fabrication tests of the additional single cell cavities will be used to evaluate the possible need to slightly adjust the deep drawing dies, in order to meet the geometry tolerances required for the fabrication of a multicell structure. After these single-cell cavity prototypes one or two five-cell cavities will be built and tested.

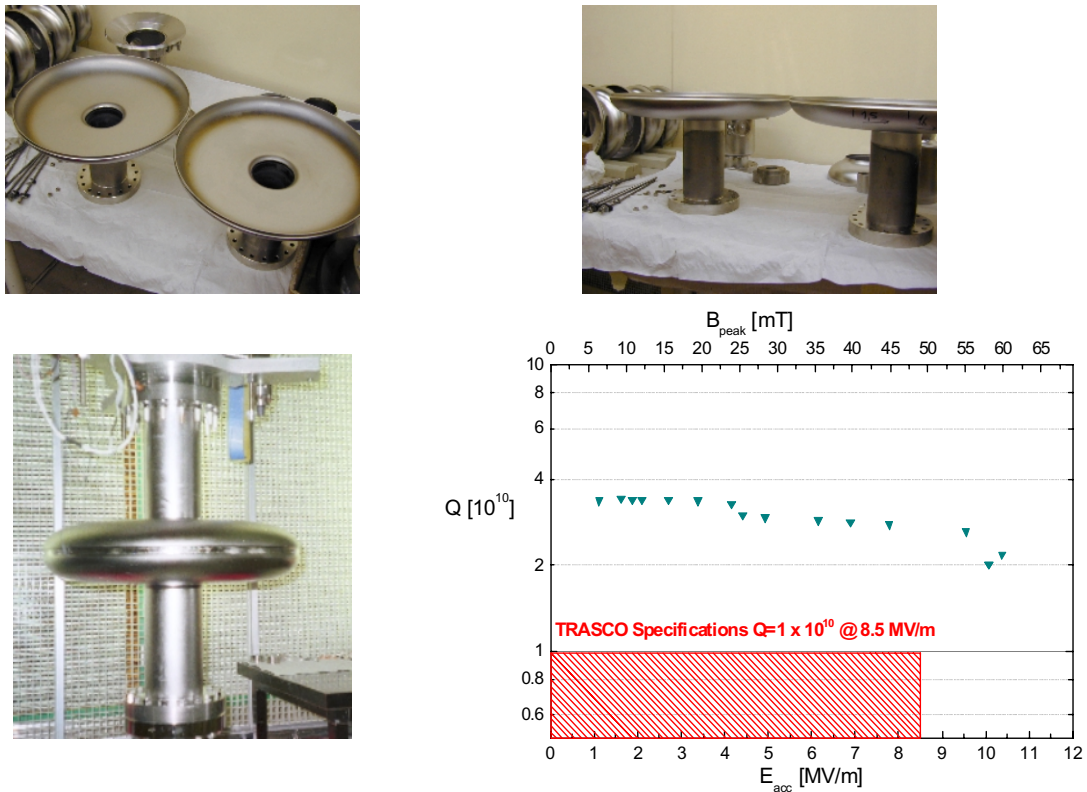


FIG. 26: Pictures and Q vs. Eacc curve of the $\beta=0.5$ bulk Nb single cell cavity.

4.2.3 The RF test bench in Milano

As part of the TRASCO_AC program, a cavity RF test bench has been set up and is under commissioning in Milano/LASA^{69,70}). The system is composed by a vertical cryostat that allows testing cavities with frequencies in the range from 500 to 800 MHz (a special insert⁶⁹) for the short beta 704.4 MHz cavities has been installed in an existing cryostat that has been used for the 500 MHz cavities of the INFN ARES program) and an RF power generator that delivers 500 W in the same band. This system however, does not allow breaking the cavity vacuum without contamination, and is ready to receive cavities for testing only if the RF antennas have already been mounted in clean conditions before sealing the cavity. Tests of the $\beta=0.5$ single cell prepared for the measurement in Saclay will be performed at the beginning of 2001. As planned for the extension of the TRASCO program, a class 100 clean room for the high pressure rinsing with ultrapure water and for the cavity preparation before the tests (mainly assembling of the RF antennas for the measurements) has been designed and will be delivered in Spring 2001, rendering the test facility fully operational. A contact with a local company for the Buffered Chemical Polishing (BCP) of the Nb cavities has been established, with the aim of acquiring complete control of the cavity preparation steps from its fabrication in Zanon to the tests in Milano.

4.2.4 Alternative schemes for cavity stiffening

While the superconducting cavity design for TRASCO is fully consistent with CW operation, in the case of the proposed pulsed operation – in view, for example, of a multipurpose machine - the Lorentz force detuning coefficient of the lowest beta cavity is probably too high. As for TESLA, an improvement of this crucial parameter is strictly related to the machine cost because of the impact on the RF power distribution and the low level RF controls.

In the framework of the MOU between INFN, CEA and IN2P3, in collaboration with the CESI laboratories in Milano and Saes Getters, we are studying and analyzing the thermal and mechanical characteristics of bimetallic niobium-copper samples produced with different deposition techniques⁷¹⁾ and thermal treatments. The sample thermal conductivity (parallel and normal to the deposition direction) has been tested at room and at cryogenic temperatures, for a modified arc technique, called “Pure-Coat”. The results are very promising, indicating a suitable conductivity, at least for the moderate-field required by the proton cavity parameters.

The mechanical properties (Interface cohesion, Young modulus, yield stress and elongation) have been measured using different techniques (pull out, four point bending, Brinell hardness test, thermal shock). The Young modulus and yield stress of the last samples are compatible with the required stiffening material specifications. The initial problem of an extreme brittleness of the deposited copper, showing an elongation before rupture of less than 0.2%, is being solved through a well-calibrated heat treatment under vacuum. A value of 2% has already been measured on the treated samples. The technological analyses are crosschecked with physical tests (SEM, Auger and XPS), to obtain a correlation between the material structure, its composition and the physical behavior. The results of the analysis are fed back for the optimization of the deposition procedures and of the surface treatments.

4.2.5 Conceptual design of the TRASCO cryomodules

The design of the cryomodule⁷²⁾ needs to be based mainly on the ADS requirements in terms of reliability and system engineering.

The cryomodule reliability is dominated by the vacuum (insulation, coupler and beam) system and by the helium cooling distribution. Fast access to the module and easy repairing, during maintenance time, complete the requirements. To achieve these requirements the cryomodules we are designing are completely independent from each other. The cryogenic transfer line runs along the modules string and the connection boxes link the modules to the He supply. Vacuum ports and RF distribution have also their own connections. Each cryomodule can be physically separated from the line with no perturbation on the working condition of the others.

To ensure good RF cavity performances the cavities need to be completely assembled in good cleaning condition (at least class 100 clean room) and all the connections to external ports have to be closed in the clean room.

The power coupler is another critical component that needs to be completely assembled and closed in the clean room. These constraints result in the necessity of considerable clearance space to fix the cold mass (that is the cavity string with the couplers and the thermal shields) in the vacuum vessel. The operation has also to prevent the alignments.

On the basis of the criteria expressed before, we have produced a conceptual design of the TRASCO cryomodule⁷²⁾. The design includes solutions that have been used and tested for the TESLA/TTF cryomodules⁷³⁻⁷⁵⁾, like the cavity sliding supports – that allow a semirigid coupler solution – or the G10 fiberglass supports – sustaining the cold cavity string and the thermal shields to a stiff room temperature frame. The vacuum vessel of the cryomodule has a large lateral flange that allows a lateral sliding of the fully assembled cold mass on the support frame, by means of rails (see FIG. 27).

The necessary assembling and alignment procedures have been identified and outlined, and follow the experience gained in the fabrication, assembly and installation of the TTF cryomodules in DESY.

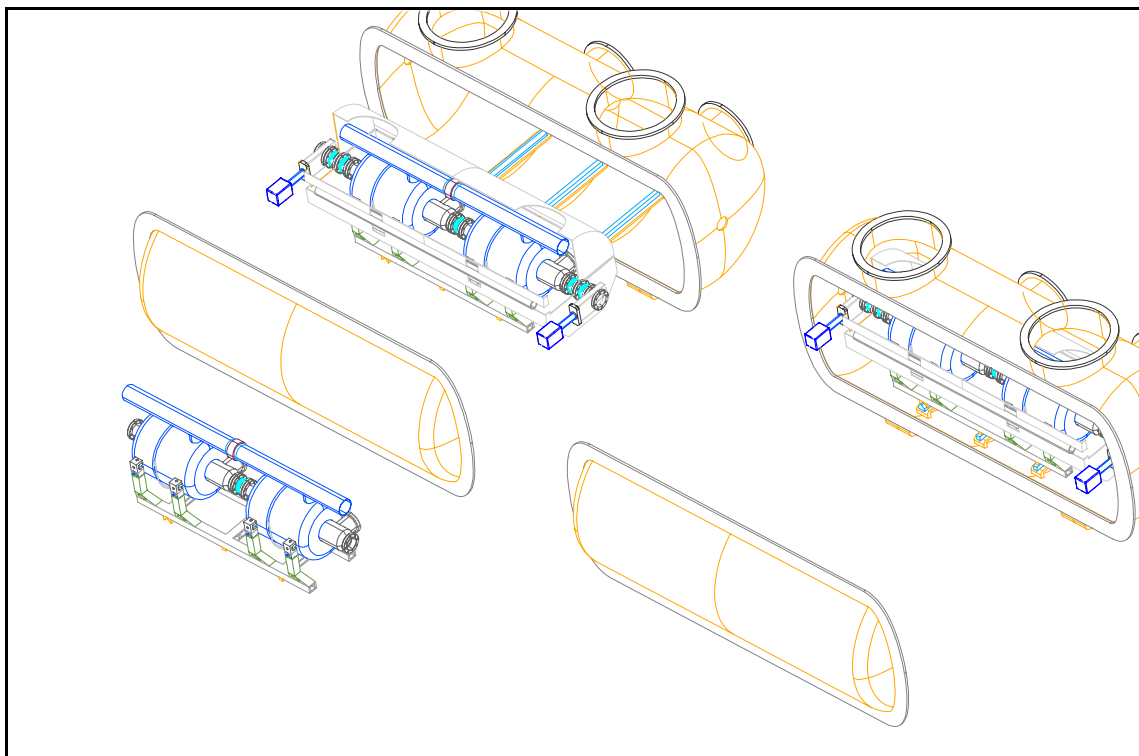


FIG. 27: The cavities string (on the left) is assembled and closed in a class 100 clean room. The system is aligned and the cold mass is assembled. The rail-sled system allows to preserve the alignment during the cold mass insertion into the vacuum vessel.

4.3 Conceptual design of the linac and beam dynamics studies

The TRASCO_AC activities for the superconducting high energy linac include the choice of a reference configuration for the linac beamline components and the beam dynamics studies aimed at the validation of the proposed configuration. The theoretical design activities have been focused mainly on two subjects:

1. The “optimal” design of the superconducting cavities^{44,45,53}).
2. The beam optics and beam dynamics studies⁴⁶⁻⁵⁰).

4.3.1 Cavity design activities

Before choosing the geometries for the fabrication of the cavity prototypes, we performed a systematic study of the electromagnetic and mechanical behavior of the cavities as a function of their shape.

In order to determine a cavity geometry that has the necessary electromagnetic and mechanical performances required by the linac design, we have used a geometry parametrization that allows easily to balance the peak electric and magnetic fields and to control the cavity mechanical properties⁴⁴). The cavity geometry is elliptical both at the equator and at the iris, and has been parametrized in a way that each geometrical parameter allows the control of a single cell electromagnetic (or mechanical) parameter.

A set of computer codes has been written in order to allow the automatic execution of standard RF cavity analysis codes (as SUPERFISH) and structural analysis codes (i.e. ANSYS) on the chosen geometry⁵³). Special tuning procedures for the inner and end-cells of a multicell cavity have been derived, with the aim of controlling the behavior of the peak fields and of the mechanical parameters during the tuning process. The structural modeling capabilities are then used to investigate the necessity of structural stiffening for the vacuum load and pressurized He operation, for mechanical tuning considerations and for the evaluation of a proper stiffening structure for the Lorentz forces and for the evaluation of the cavity structural eigenmodes, in order to investigate the possibility of exciting microphonics vibrations.

With the aid of these analyses and tools, and in close collaboration with the CEA/Saclay and IN2P3/Orsay groups working at the design of the ASH proposal⁷⁶), we defined the cavity shapes for the TRASCO (and ASH) cavities⁵¹). These are the shapes used for the cavity prototyping activities in Milano and in Saclay. The main cavity geometrical and electromagnetic parameters are reported in TAB. 5, while the geometry of the multicell cavities and the electric field lines are shown in FIG. 28.

As it can be seen from the figure, the beam tube at the coupler end of the cavity has a bigger aperture than the cell irises, in order to improve the main power coupling. The lowest beta cavity has the worst mechanical stiffness (both with respect to Lorentz forces and vacuum load), and here the use of an elliptical shaped equator, which better distributes

stresses along the cavity walls, simplifies the stiffening structure. The other cavities have a round shape in order to ease the cell fabrication process. A stiffening structure for the beta 0.5 cavity by means of a TESLA-like welded ring, allows to reduce the Lorentz force detuning at the operating accelerating field from about 1 KHz to 620 Hz. The Lorentz force detuning of the higher beta cavities is well below 300 Hz, and hence the cavities do not require a stiffening structure. The accelerating fields used in forces calculations correspond to the maximum nominal peak magnetic field of 50 mT on the cavity walls.

TAB. 5: Main cavity parameters.

Geometrical Parameters			
Cavity synchronous beta	0.50	0.68	0.86
Number of cells	5	5	6
Cell geom. length [mm]	100	140	180
Geometrical beta	0.470	0.658	0.846
Full Cavity Length [mm]	900	1100	1480
Iris diameter [mm]	80	90	100
Tube \varnothing at coupler [mm]	130		
Internal wall angle, α [$^\circ$]	5.5	8.5	8.5
Equator ellipse ratio, R	1.6	1	1
Iris ellipse ratio, r	1.3	1.3	1.4
Full cavity electromagnetic Parameters			
Max. $E_{\text{peak}}/E_{\text{acc}}$	3.59	2.61	2.36
Max. $B_{\text{peak}}/E_{\text{acc}}$	5.87	4.88	4.08
Cell to cell coupling [%]	1.34	1.10	1.28
R/Q [Ohm]	159	315	598

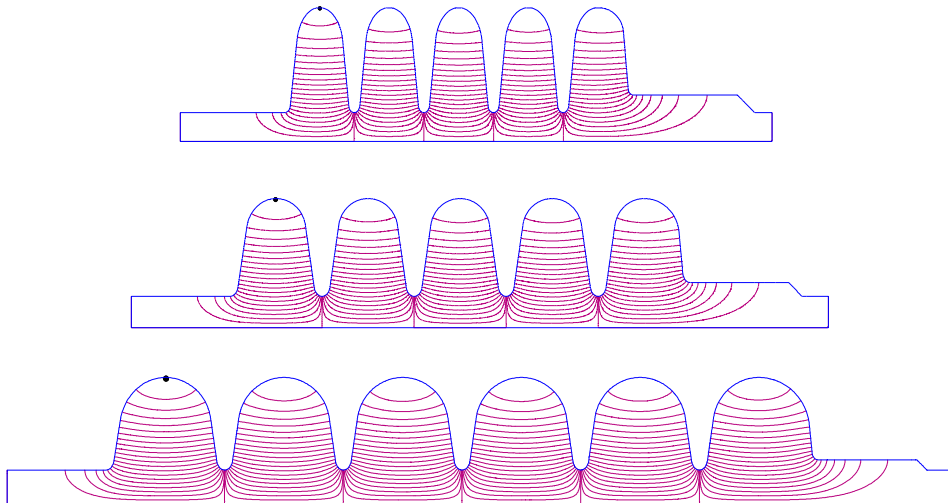


FIG. 28: The three multicell cavities designed for the TRASCO linac.

4.3.2 Linac design and simulation codes

A few guidelines imposed by either technological limitations or first order beam optics considerations have been followed in the definition of the linac reference design^{47,48,50}, and it is worth summarizing them in the following paragraphs. For sake of simplicity in the following discussion only the 704.4 MHz design⁵⁰ will be presented, but more details on the design at the 352.2 MHz LEP II frequency are in the references^{47,48}.

The energy range from about 90-100 MeV up to 1-2 GeV can be efficiently covered with three sections, i.e. with three different cavity types. A larger number of sections would imply a wider cavity R&D activity for a smaller number of production cavities, while a smaller one would lead to inefficient use of the cavity transit time factor.

The transition energies between the sections have been (loosely) set to 200 MeV and 500 MeV, independently on the optimization of the input energy (say from 85 to 100 MeV) and from the output energy (from 1 to 2 GeV).

The number of cavities per section has been derived using a conservative value of 50 mT for the peak surface magnetic field.

The number of cells has been chosen to be 5 in the two lowest beta sections and 6 in the highest beta section.

The transverse focusing lattice is formed by an array of quadrupole doublets, with the cavity cryostats in the long drift between quads. The cryostats contain 2 cavities in the two lowest beta sections and 4 cavities in the highest beta. With these choices the doublet periodicity in the three sections is 4.2, 4.6 and 8.5 m, respectively, and the quadrupole doublets are located in a 1.6 m warm section between the cryomodules.

The cavity fields and quadrupole gradients are chosen so to keep the zero current transverse and longitudinal phase advances smaller than 90 degrees along the whole linac.

The cavities in the first section operate at an average accelerating field of 7.4 MV/m and 20 lattice periods bring the beam energy to the transition to the second section (roughly 200 MeV). Here 27 lattice periods with cavities operating at an average accelerating field of 9.8 MV/m bring the beam to the last section (at an energy of nearly 500 MeV). At the entrance of the last section the cavity gradient is reduced to achieve a smooth matching of the longitudinal beam tune and finally the last part of the linac is operated at a constant energy gain of 11.4 MeV per cavity. The cavities in the last section operate at an average accelerating gradient of 11.8 MV/m. With 13 lattice periods of the highest beta section the beam energy has reached 1 GeV, for a section length of 110.5 m. Additional 22 lattice periods can increase the beam energy to 2 GeV. TAB. 6 lists the main parameters of the linac sections for the 1 GeV and the 2 GeV linac cases.

The beam line design and matching has been investigated and analyzed with a number of different beam optics codes, either standard design codes available in the accelerator community or tools that have been developed for the proton linac studies in Milano or Saclay³⁹⁻⁴³. These codes allowed to set the desired transverse phase advances

law, and the matching conditions at the linac entrance - and between the linac sections – that are needed to minimize the emittance growth that can lead to undesired beam losses. As it can be seen from FIG. 29 for the case of an average current of 20 mA, a special care has been used in setting the transverse phase advances to avoid first order resonance between the longitudinal and transverse tunes, which always lead to very fast emittance exchanges between the two planes.

TAB. 6: Main SC linac section parameters.

	Section 1	Section 2	Section 3	
			1 GeV	2 GeV
Section β_s	0.50	0.68	0.86	
Section Length [m]	84	124.2	110.5	297.5
Input Energy [MeV]	85	200	500	
Focussing Period [m]	4.2	4.6	8.5	
# Focussing Periods	20	27	13	35
Max Gain/Cavity [MeV]	3.3	6.0	11.4	
Max Eacc [MV/m]	8.5	10.2	12.3	
# Cells/Cavity	5	5	6	
# Cavities/Section	40	54	52	140
# Cavities/Cryomodule	2	2	4	
# Cryomodule/Klystron	1	1	1	
Max RF/Coupler [kW]	66	120	228	

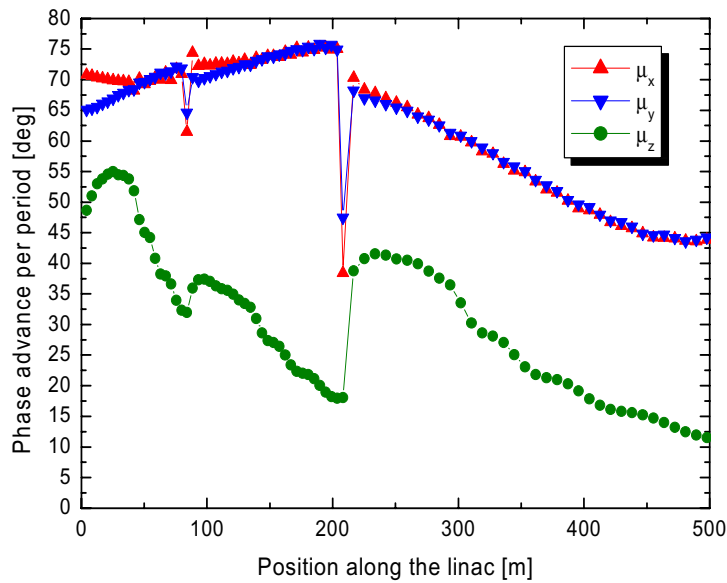


FIG. 29: Matched phase advances for the 2 GeV linac.

We have specially written a beam dynamics code⁴⁶⁾ for the simulations of the SC TRASCO linac (SCDyn), which advances particles in phase steps through the beam line elements of the linac. Analytical maps are used for the particle propagation in drifts and quadrupole elements, whereas a direct integration along the on-axis field of the RF cavities is performed (with a second order off-axis expansion to account for transverse focusing effects). The reason for using such a cavity modeling technique, which is more cumbersome on the computational point of view with respect to a standard “thin gap” approximation, lies in the behavior of the cavity transfer matrix elements as a function of the particle energy. As we have shown in reference⁴⁸⁾, a cavity model based on a single thin gap fails to reproduce the cavity transfer matrix elements except for the particles at the nominal energy of the reduced beta structure.

The space charge calculations in SCDyn are performed with a cloud in cell charge deposition scheme and a 3D V-cycle multigrid Poisson solver in the beam rest frame.

We have extensively used SCDyn for the validation of the TRASCO linac design, and made comparisons with other beam dynamics codes – notably Parmila (Los Alamos) and Partran (Saclay).

In FIG. 30 we show the behavior of the rms beam sizes along the beam line, for a 1 GeV linac case, corresponding to the same matched case of the previous figure. The beam sizes shown in the figure are the rms envelopes evaluated from the SCDyn multiparticle simulations. The sharp increase of the matched beam size in the last section, due to the big difference between the lattice periods (4.6 m in the second section and 8.5 m in the third), does not lead to any beam emittance increase, as it will be shown in the following figures, but allows a drastic increase of the linac filling factor.

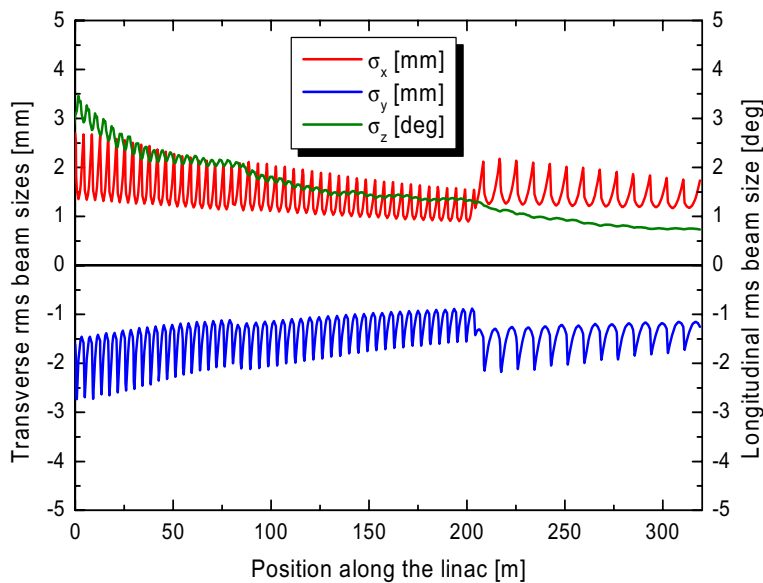


FIG. 30: rms matched beamsizes in the 1 GeV linac, from the SCDyn simulations.

The next figure shows the rms normalized emittances along the linac. The top part of the figure shows the relative rms emittance variation from the initial value. A small emittance exchange between the planes can be seen, leading to a 5% increase of the longitudinal emittance and a 2% decrease of the transverse. Most of the emittance exchange occurs in the first section, possibly due to the non-stationary nature of the initial distribution under the space charge forces (we used a 6D uniform waterbag). The bottom part of the figure displays the behavior of the transverse and longitudinal beam emittances along the linac beamline.

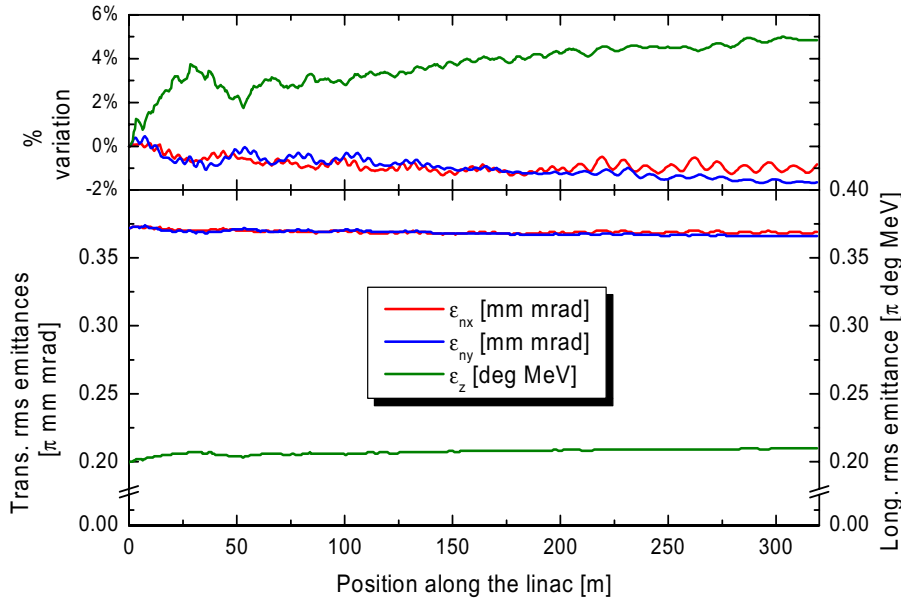


FIG. 31: Bottom plot: rms beam emittances along the linac.

Top plot: variation of the beam emittances with respect to the initial value.

It is worth pointing out that we did not only achieve an rms beam matching along the linac, but indeed the particles are perfectly matched up to the 90% beam size, and only the last 1% of the simulated beam distribution experience small bounded mismatched oscillations. The ratio between the beamline aperture ratio and the outermost particle position in the beam is always greater than 10, whereas the ratio of the aperture to the rms beamsizes exceeds 25 along the linac.

Finally, the next figure shows the phase spaces of the output beam from the SCDyn simulations, at 1 GeV, for a 50,000 particles simulation. The two ellipses drawn on the phase spaces indicate the rms emittance and 4 times the rms. The characteristic rectangular shape of a space charge dominated beam can be clearly seen in the horizontal phase space (top left). Mismatched case up to a mismatch factor of 30% have shown the onset of filamentation effects that increase the beam emittances, but no evidence of unbounded orbits could be seen from the simulations.

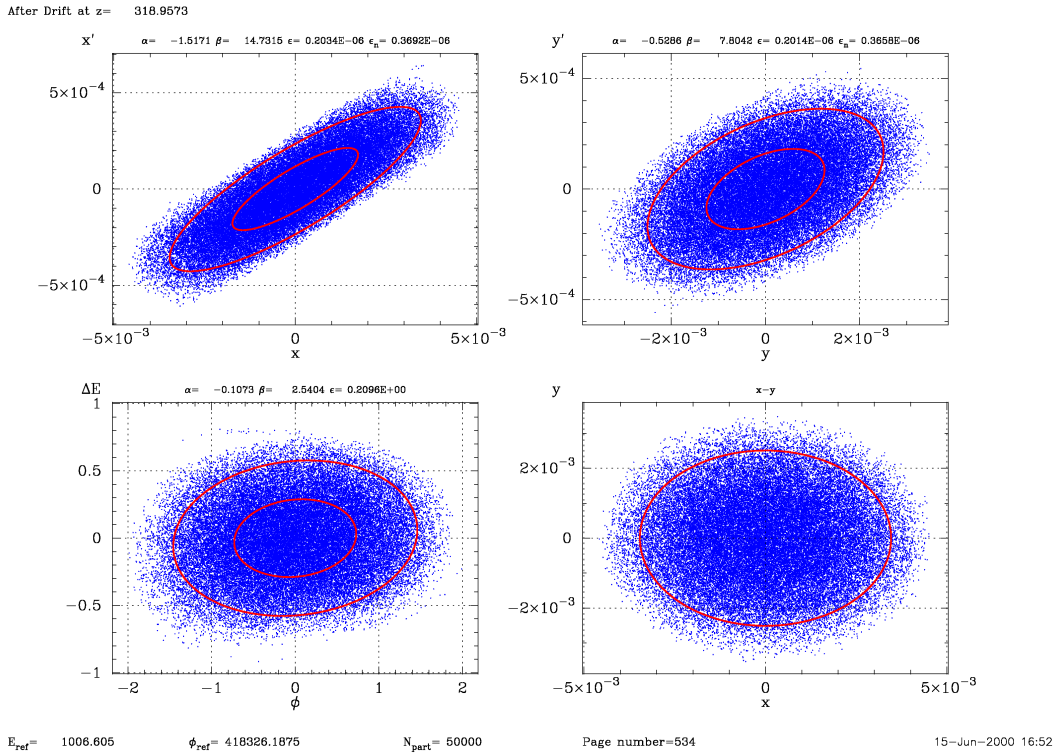


FIG. 32: The phase spaces of the output beam (for a 50 k particle simulation).

5 CONCLUSIONS

We have described here the status of the activities of the TRASCO_AC program. We have outlined a reference solution for all the components of the accelerator and we have achieved significant experimental results. A prototype of the TRIPS source has delivered its first beam in LNS, with specifications close to the design values. An aluminum model of the RFQ has been built and tested, while the technological model of the RFQ and a prototype reentrant cavity are in fabrication. Both a five-cell high beta, 352.2 MHz, Nb/Cu cavity - built and tested at CERN - and a low beta, 704.4 MHz, bulk Nb single-cell cavity - built by Zanon and tested at Saclay - have met the design specifications in experimental tests.

6 REFERENCES

- (1) See <http://jkj.tokai.jeaeri.go.jp>
- (2) See <http://apt.lanl.gov>
- (3) “Research and Industrial Programmes on ADS in Italy”, M. Napolitano, in *Proceedings of the 1998 OECD/NEA Workshop on "Utilization and Reliability of High Power Accelerators"*, Tokai-Mura, Japan, p. 137
- (4) C. Rubbia et al., "Conceptual Design of a Fast Operated High Power Energy Amplifier". CERN/AT/95-44(ET). September 1995; C. Rubbia et al., "Fast Neutron Incineration in the Energy Amplifier as Alternative to Geological Storage: the Case of Spain". CERN/LHC/97-01(EET). February 1997
- (5) “A microwave source for high current of protons”, G.Ciavola, S.Gammino, Report LNS 21-10-96
- (6) “Improvement of beam emittance of the CEA high intensity proton source SILHI”, R. Gobin, P.-Y. Beauvais, R. Ferdinand, P.-A. Leroy, L. Celona, G. Ciavola, and S. Gammino, in *Review of Scientific Instruments*, Vol **70** n.6, (1999), p. 2652
- (7) “Emittance improvement of the electron cyclotron resonance high intensity light ion source proton beam by gas injection in the low energy beam transport”, P.-Y. Beauvais, R. Ferdinand, R. Gobin, J. M. Lagniel, P.-A. Leroy, L. Celona, G. Ciavola, and S. Gammino, B. Pottin, J. Sherman, in *Review of Scientific Instruments*, Vol **71** n.3, (2000), p. 1413
- (8) “Status and new developments of the high intensity electron cyclotron resonance source light ion continuous wave, and pulsed mode”, J.-M. Lagniel, P.-Y. Beauvais, D. Bogard, G. Bourdelle, G. Charruau, O. Delferriere, D. De Menezes, A. France, R. Ferdinand, Y. Gauthier, R. Gobin, F. Harrault, J.-L. Jannin, P.-A. Leroy, I. Yao, P. Ausset, B. Pottin, and N. Rouviere, L. Celona and S. Gammino, in *Review of Scientific Instruments*, Vol **71** n.2, (2000), p. 830
- (9) “ACTIVITY REPORT ON SILHI ION SOURCE (13 September - 16 October 1998)”, L. Celona, R. Gobin, Report DAPNIA/SEA/IPHI 98-69
- (10) “SECOND ACTIVITY REPORT ON SILHI ION SOURCE (November 22 - December 18 1998)”, L. Celona, R. Gobin, P.Y. Beauvais, P.A. Leroy, DAPNIA/SEA/IPHI 98-79
- (11) “THIRD ACTIVITY REPORT ON SILHI ION SOURCE (June 07 - July 02, 1999)”, L. Celona, S. Gammino, R. Gobin, O. Delferrière, R. Ferdinand, D. De Menezes, N. Pichoff, J. Sherman, DAPNIA/SEA/IPHI 99-52
- (12) “TRIPS: The high intensity proton source for the TRASCO project”, L. Celona, G. Ciavola, S. Gammino, R. Gobin and R. Ferdinand, in *Review of Scientific Instruments*, Vol **71** n.2, (2000), p. 771
- (13) “Installation of TRIPS at INFN-LNS”, G. Ciavola, L. Celona, S. Gammino, S. Marletta, C. Campisano, in *Proceedings of EPAC 2000*, Vienna, Austria, p. 1592
- (14) “The DTL approach for a 100 MeV CW linac”, A.Pisent, M. Comunian, G. Fortuna, A. Lombardi, M.F. Moio, November 5, 1996, INFN/LNL Report
- (15) “Beam dynamics issues of a 100 MeV superconducting proton linac”, in *Proceedings of the RF SC Workshop 97*, Abano Terme, Italy

- (16) “A 100 MeV superconducting proton linac: beam dynamics issues”, M. Comunian, A. Facco, A. Pisent, in *Proceedings of the LINAC 98*, Chicago, United States, p. 64
- (17) “TRASCO 100 MeV high intensity proton linac”, A. Pisent, M. Comunian, A. Facco, M. Pasini, V. Zviagintsev, L.Celona, G. Ciavola, S. Gammino, G. Lamanna, in *Proceedings of EPAC 2000*, Vienna, Austria, p. 857
- (18) “A superconductive, low beta single gap cavity for a high intensity proton linac”, A. Facco, V. Zviagintsev, B. M. Pasini, in *Proceedings of the Linac 2000*, United States, Contribution THD11
- (19) “Test of a radio-frequency quadrupole cold model”, G. V. Lamanna, A. Lombardi, A. Pisent, in *Proceedings of the PAC99*, New York, United States, p. 3522
- (20) “Equivalent lumped circuit study for the field stabilization of a long four-vanes RFQ”, A. Pisent, R. Celentano, R. Zennaro, in *Proceedings of the LINAC 98*, Chicago, United States, p. 968
- (21) “Transmission line analysis of coupled RFQ's”, A. Pisent, TRASCO Note 01/99, LNL
- (22) “TRASCO RFQ design”, M.Comunian, G.Lamanna, A.Pisent, TRASCO Note 01/00, LNL
- (23) “TRASCO RFQ Design”, M. Comunian, A. Pisent, G.V. Lamanna, in *Proceedings of EPAC 2000*, Vienna, Austria, p. 927
- (24) “TRASCO RFQ”, A.Pisent, M. Comunian, A. Palmieri, G.V.Lamanna, D.Barni, in *Proceedings of the Linac 2000*, United States, Contribution THD02
- (25) “Frequency map analysis of an intense mismatched beam in a FODO channel”, A. Bazzani, M. Comunian, A. Pisent, Report LNL-INFN 127/98
- (26) “Frequency map analysis for beam halo formation in high intensity beams”, A.Bazzani, M.Comunian, A.Pisent, in *Proceedings of the PAC99*, New York, United States, p. 1773
- (27) “Frequency map analysis of beam halo formation in a high intensity proton linac”, A. Pisent, M. Comunian, A. Bazzani, in *Proceedings of EPAC 2000*, Vienna, Austria, p. 1327
- (28) “3D solution of the Poisson-Vlasov equations for a line of FODO cells”, G. Turchetti, S. Rambaldi, A. Bazzani, M. Comunian, A. Pisent, in *Proceedings of the International Computational Accelerator Physics 2000*, Darmstadt, Germany
- (29) “A High Current Proton Linac with 352 MHz SC Cavities”, C. Pagani, G. Bellomo, P. Pierini, in *Proceedings of LINAC96*, Geneva, Switzerland, MOP23
- (30) “A high current superconducting proton linac for an accelerator driven transmutation system”, G. Bellomo, C. Pagani, P. Pierini, G. Travish, D. Barni, A. Bosotti, R. Parodi, in *Proceedings of the PAC97*, Vancouver, Canada
- (31) “A 100-1600 MeV high current SC proton linac for waste transmutation and energy amplification”, C. Pagani, G. Bellomo, P. Pierini, D. Barni, A. Bosotti, A. Martino, R. Parodi, S. Visonà, in *Proceedings of the RF SC Workshop 97*, Abano Terme, Italy
- (32) “Superconducting Accelerators for Nuclear Waste Transmutation”, C. Pagani, D. Barni, G. Bellomo, R. Parodi, P. Pierini, in *Proceedings of the Applied Superconductivity Conference 98*, Palm Desert, United States

- (33) “Status of the INFN high current SC proton linac for nuclear waste transmutation”, C. Pagani, D. Barni, G. Bellomo, R. Parodi, P. Pierini, in *Proceedings of the LINAC 98*, Chicago, United States, p. 1013
- (34) “Activities on the high current SC proton linac for the TRASCO project”, Carlo Pagani, in *Proceedings of the 1998 OECD/NEA Workshop on "Utilization and Reliability of High Power Accelerators"*, Tokai-Mura, Japan, p. 263.
- (35) “High power CW superconducting linacs for nuclear waste processing”, C. Pagani and P. Pierini, in *Proceedings of the 1999 Cryogenic Engineering Conference*, Montreal, Canada
- (36) “Scientific issues and status of the Franco-Italian collaboration of the SC linear accelerator for ADS”, C. Pagani, in *Proceedings of the 1999 OECD/NEA Workshop on "Utilization and Reliability of High Power Accelerators"*, Aix-en-Provence, France
- (37) “Review of Superconducting RF Technology for High-Power Proton Linacs”, K. C. D. Chan, H. Safa, C. Pagani, M. Mizumoto, in *Proceedings of the RF SC Workshop 99*, Los Alamos, United States
- (38) “Upgrade of the TRASCO SC linac design @700 MHz”, C. Pagani, D. Barni, G. Bellomo, A. Bosotti, P. Michelato, G. Penco, P. Pierini, G. Varisco, G. Gemme, R. Parodi, in *Proceedings of EPAC 2000*, Vienna, Austria, p. 957
- (39) “1st Meeting on High Power Superconducting Proton Accelerator for Nuclear Waste Transmutation”, Milano-LASA, February 23-24, 1999
- (40) “2nd Meeting on High Power Superconducting Proton Accelerator for Nuclear Waste Transmutation”, IPN Orsay, June 28-29, 2000
- (41) “3rd Meeting on High Power Superconducting Proton Accelerator for Nuclear Waste Transmutation”, CEA Saclay, October 18-19, 1999
- (42) “4th Meeting on High Power Superconducting Proton Accelerator for Nuclear Waste Transmutation”, Milano-LASA, January 27-28, 2000
- (43) “5th Meeting on High Power Superconducting Proton Accelerator for Nuclear Waste Transmutation”, IPN Orsay, 2000
- (44) “SC beta graded cavity design for a proposed 350 MHz linac for waste transmutation and energy production”, D. Barni, A. Bosotti, C. Pagani, P. Pierini, S. Visonà, G. Gemme, R. Parodi, in *Proceedings of EPAC 1998*, Stockholm, Sweden, p. 1870
- (45) “SC Cavity design for the 700 MHz TRASCO linac”, D. Barni, A. Bosotti, G. Ciovati, C. Pagani, P. Pierini, in *Proceedings of EPAC 2000*, Vienna, Austria, p. 2019
- (46) “A multigrid-based approach to modeling a high current superconducting linac for waste transmutation”, Paolo Pierini, in *Proceedings of the International Computational Accelerator Physics 98*, Monterey, United States
- (47) “Beam dynamics in a proposed 350 MHz SC linac for nuclear waste transmutation and energy production”, G. Bellomo, P. Pierini, in *Proceedings of EPAC 1998*, Stockholm, Sweden, p. 1103
- (48) “Beam Dynamics in a high current SC proton linac for nuclear waste transmutation”, G. Bellomo, P. Pierini, in *Proceedings of the LINAC 98*, Chicago, United States, p. 153

- (49) “A multigrid-based beam dynamics code for high current proton linacs”, P. Pierini, G. Bellomo and C. Pagani, in *Proceedings of the PAC99*, New York, United States, p. 1776
- (50) “Validation of the 700 MHz TRASCO SC linac design by multiparticle simulations”, P. Pierini, G. Bellomo, C. Pagani, in *Proceedings of EPAC 2000*, Vienna, Austria, p. 1324
- (51) “704 MHz superconducting cavities for a high intensity proton accelerator”, J.L. Biarrotte, H. Safa, J.P. Charrier, S. Jaidane, H. Gassot, T. Junquera, J. Lesrel, G. Ciovati, P. Pierini, D. Barni, C. Pagani, in *Proceedings of the RF SC Workshop 99*, Los Alamos, United States
- (52) “Production and test of the prototype $\beta= 0.85$ five cell cavity for the TRASCO project”, E. Chiaveri, R. Losito, S. Calatroni, A. Dacca, G. Gemme, R. Parodi, D. Barni, A. Bosotti, C. Pagani, G. Varisco, in *Proceedings of the RF SC Workshop 99*, Los Alamos, United States
- (53) “Cavity design tools and applications to the TRASCO project”, P. Pierini, D. Barni, A. Bosotti, G. Ciovati, C. Pagani, in *Proceedings of the RF SC Workshop 99*, Los Alamos, United States
- (54) “Study of microwave coupling in electron cyclotron resonance ion sources and microwave ion sources”, L. Celona, G. Ciavola and S. Gammino in *Review of Scientific Instruments*, Vol 69 n.2, (1998), p. 1113
- (55) “Ionization efficiency measurements with the microwave discharge ion source MIDAS”, L. Celona, S. Gammino, G. Ciavola, F. Chines, S. Marletta, E. Messina in *Proceedings of EPAC 2000*, Vienna, Austria, p. 1601
- (56) “A 6.7 MeV CW RFQ Linac” D. Schrage et al. in *Proceedings of the PAC 97*, Vancouver, CA, p. 1093.
- (57) “RFQ Design Codes”, K.R. Crandall, J.H. Billen, R.S. Mills, D.L. Schrage, R.H. Stokes, G.H. Neuschaefer, T.P. Wangler, and L.M. Young, *LA-UR-96-1836*.
- (58) “IPHI-RFQ reliability approach”, R. Ferdinand, R. Duperrier, in *Proceedings of Second Workshop on Utilizations and Reliability of High Power Accelerators*, Aix-en-Provence, France, 22-24 November 1999.
- (59) “Tuning the LEDA RFQ 6.7 MeV Accelerator”, L.M. Young, L.J. Rybarczyk, in *Proceedings of the 1998 International Linac Conference*, Argonne, USA p. 270
- (60) G. Geschonke, private communication
- (61) “Low cost High Power UHF MOSFET Amplifier”, T. Ruan et al., in *Proceedings of the 7th Annual Workshop on European Synchrotron Light Sources, ESLS 7*, Berlin, Germany, November 1999
- (62) “Completion of the LNL Bulk Niobium Low Beta Quarter Wave Resonators”, A. Facco, V. Zviagintsev, in *Proceedings of the 9th Workshop on RF Superconductivity*, Santa Fe, USA, 1999
- (63) “Research and Development in the Field of SCRF at INFN-LNL”, A.M. Porcellato et al., in *Proceedings of the 9th Workshop on RF Superconductivity*, Santa Fe, USA, 1999
- (64) “Fast Damping in Beam Envelope Oscillation Amplitudes of mismatched high intensity beams”, V. Variale, T. Clauser, V. Stagno, in *Proceedings of the EPAC 2000*, Vienna, 26 - 30, 2000

- (65) “Production by Industry of a Large Number of Superconducting Cavities: Status and Future, E. Chiaveri, in *Proceedings of the RF SC Workshop 1995*, Gif Sur Yvette, France, p. 181
- (66) “TESLA Test Facility Linac – Design Report”, Editor D.A. Edwards, DESY Print, March 1995, TESLA 95-01
- (67) “Status and Perspectives of the SC Cavities for TESLA”, C. Pagani, *Advances in Cryogenic Engineering*, V **45A**, 2000, p. 881
- (68) “The CERN Nb/Cu Programme for Reduced- β Superconducting Cavities”, E. Chiaveri, *Workshop on R&D on Superconducting Proton Linac*, Saclay, France, 2000.
- (69) “Beta tunable 700 MHz insert with natural convection precooling”, D. Barni, C. Gesmundo, C. Pagani, G. Varisco, in *Proceedings of the RF SC Workshop 99*, Los Alamos, United States
- (70) “Superconducting RF activities at INFN Milano-LASA”, C. Pagani, in *Proceedings of the RF SC Workshop 99*, Los Alamos, United States
- (71) “A New Fabrication and Stiffening Method of SRF Cavities, S. Bousson et al., in *Proceedings of the EPAC 1998*, Stockholm, Sweden, p. 1849
- (72) “Conceptual design of the cryomodule for the TRASCO SC linac”, D. Barni and C. Pagani, in *Proceedings of EPAC 2000*, Vienna, Austria, p. 2022
- (73) “Construction, Commissioning And Cryogenic Performances Of The First TESLA Test Facility (TTF) Cryomodule”, C. Pagani, J.G. Weisend II, R. Bandelman, D. Barni, A. Bosotti, G. Grygiel, H. Kaiser, U. Knopf, R. Lange, F. Loeffler, P. Pierini, O. Peters, B. Petersen, D. Sellmann, S. Wolff, in *Advances in Cryogenic Engineering*, V **43A**, 1998, p. 87
- (74) “Towards The Third Generation Of TTF Cryomodules”, D. Barni, C. Pagani, P. Pierini, TESLA Report, DESY TESLA 98-16
- (75) “The TESLA Test Facility (TTF) Cryomodule: A Summary Of Work To Date”, J. G. Weisend II , C. Pagani, R. Bandelmann, D. Barni, A. Bosotti, G. Grygiel, R. Lange, P. Pierini, B. Petersen, D. Sellmann, S. Wolff, in *Proceedings of the 1999 Cryogenic Engineering Conference*, Montréal, Canada, 1999
- (76) “Superconducting Proton Linac for Waste Transmutation”, H. Safa, in *Proceedings of the RF SC Workshop 99*, Los Alamos, United States
- (77) “RF Superconductivity at INFN-Genoa”, R. Parodi, in *Proceedings of the RF SC Workshop 99*, Los Alamos, United States
- (78) “Analysis of the losses of superconducting cavities as a function of field and temperature”, R. Ballantini, A. Daccà, G. Gemme, R. Parodi, in *Proceedings of the RF SC Workshop 99*, Los Alamos, United States